

## THE STATE OF THE CALIFORNIA CURRENT IN 1998–1999: TRANSITION TO COOL-WATER CONDITIONS

THOMAS L. HAYWARD  
Marine Life Research Group  
Scripps Institution of Oceanography  
University of California, San Diego  
9500 Gilman Drive  
La Jolla, California 92093-0227  
thayward@ucsd.edu

REGINALDO DURAZO  
UABC—Facultad de Ciencias Marinas  
Apartado Postal 453  
Ensenada, B.C.  
México

TOM MURPHREE  
Department of Meteorology  
Naval Postgraduate School  
Monterey, California 93943

TIM R. BAUMGARTNER  
Centro de Investigación Científica y  
Educación Superior de Ensenada  
División de Oceanología  
Km. 107 Carretera Tijuana-Ensenada  
Ensenada, B.C.  
México

GILBERTO GAXIOLA-CASTRO  
Centro de Investigación Científica y  
Educación Superior de Ensenada  
División de Oceanología  
Km. 107 Carretera Tijuana-Ensenada  
Ensenada, B.C.  
México

FRANKLIN B. SCHWING  
Pacific Fisheries Environmental Laboratory  
National Marine Fisheries Service, NOAA  
1352 Lighthouse Avenue  
Pacific Grove, California 93950-2097

MIA J. TEGNER  
Marine Life Research Group  
Scripps Institution of Oceanography  
University of California, San Diego  
9500 Gilman Drive  
La Jolla, California 92093-0227

DAVID M. CHECKLEY  
Marine Life Research Group  
Scripps Institution of Oceanography  
University of California, San Diego  
9500 Gilman Drive  
La Jolla, California 92093-0227

K. DAVID HYRENBACH,  
ARNOLD W. MANTYLA, MICHAEL M. MULLIN  
Marine Life Research Group  
Scripps Institution of Oceanography  
University of California, San Diego  
9500 Gilman Drive  
La Jolla, California 92093-0227

PAUL E. SMITH  
Southwest Fisheries Science Center  
National Marine Fisheries Service, NOAA  
P.O. Box 271  
La Jolla, California 92038

### ABSTRACT

This report reviews and provides a preliminary interpretation of recent observations made by CalCOFI (California Cooperative Oceanic Fisheries Investigations) and other programs sampling the coastal waters of the Californias. Since this is a continuation of a series of annual reports, the emphasis here is upon observations made during the past 18 months, but longer-term trends must also be considered. The major change in oceanographic structure in the past year was the transition from strong El Niño conditions in early 1998 to cool-water, La Niña conditions in early 1999. Ecosystem structure also showed large changes during this period. Phytoplankton abundance during 1998, as indicated by chlorophyll concentration, was typical of the values seen during the last decade, but it appeared to be increasing in early 1999 in association with the transition to cool-water conditions. Macrozooplankton biomass during 1998 continued the long-term trend of low values which have been seen since the mid-1970s regime shift, and El Niño-related changes were superimposed upon this trend. The 1999 macrozooplankton data are not yet available to assess whether biomass is increasing. Observations made at coastal shore stations, in southern California kelp forest communities, in central and northern California, and in Baja California, Mexico, are considered in order to place the CalCOFI observations in a larger regional context. Because this year marks the fiftieth an-

niversary of the CalCOFI program, we use the discussion to consider future directions for the time-series program and how the CalCOFI data can be put to greater use at the regional, state, and national level.

### INTRODUCTION

This is a continuation in a series of reports (e.g., Hayward et al. 1996; Schwing et al. 1997; Lynn et al. 1998) which present and synthesize recent observations in the California Current system. The emphasis is upon data collected during 1998 and 1999. The 1998–99 period was marked by rapid and remarkable changes in physical and ecosystem structure in the study region. Winter and spring of 1998 was a period of strong El Niño conditions in physical and biological structure. The physical influence of El Niño declined during the summer and fall of 1998, and there was a transition to cool-water conditions during the winter of 1998 and the spring of 1999.

Oceanographic programs to the south—sampling off northern Baja California, Mexico—and to the north—sampling off Monterey and the central California coast—are making observations that help to put the CalCOFI time series in a larger regional context, and that allow the influence of El Niño to be examined on larger spatial scales. Observations made at coastal shore stations and in kelp forest communities are being related to CalCOFI time-series observations in order to determine

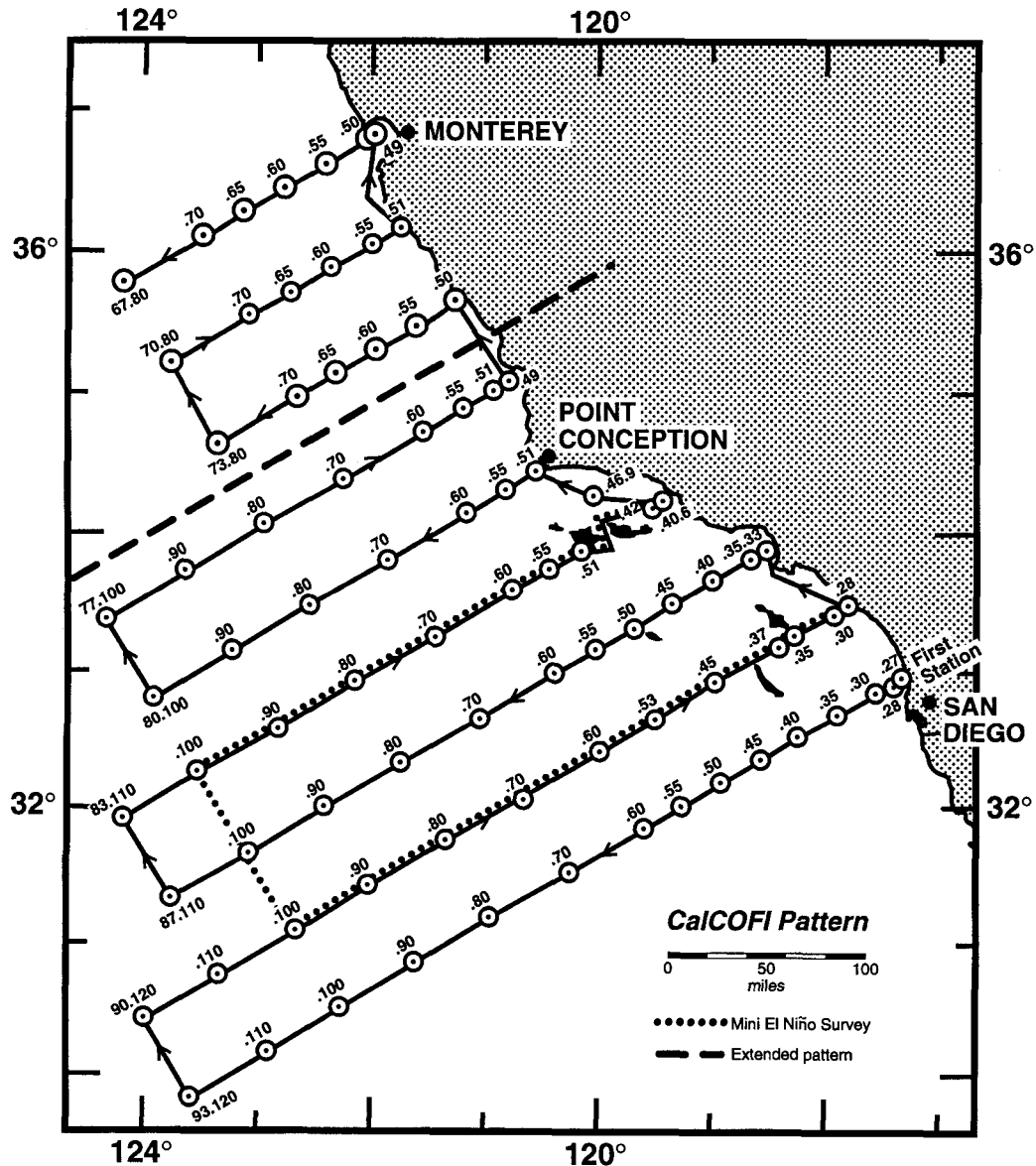


Figure 1. CalCOFI station patterns. The regular 66-station station pattern occupied by CalCOFI since 1985 (lines 77, 80, 83, 87, 90, and 93) is connected with a solid line. The stations for the mini El Niño cruises on lines 83 and 90 are shown with a dotted line. The area of additional underway sampling north of the regular pattern is above the dashed line (lines 67, 70, and 73).

if these regions respond in a similar way to changes in environmental structure and whether the higher-frequency, longer temporal coverage and greater spatial coverage of the coastal shore station data can be used to make inferences about structure in the offshore waters of the California Current.

As in past reports, we highlight the observations and findings of a few of the new types of techniques that are being evaluated in CalCOFI, and the results of some of the cooperative research programs. The 1998–99 period was also marked by the continuation of the process of implementing new observational approaches in the CalCOFI time series. Observations with CUFES (continuous underway fish egg sampler) provide greatly improved spatial resolution of the pattern of fish spawning

during this period of rapid change. Implementation of the OPC (optical plankton counter) is providing the basis to determine whether the size spectrum and/or depth distribution of the plankton changes during this period of rapid environmental change.

#### DATA AND SAMPLING

The observations presented here were obtained from several sources. CalCOFI observations include data from the quarterly survey cruises and from the additional “mini El Niño” cruises which sampled lines 90 and 83 on RV *Robert Gordon Sproul* from December 1997 to January 1999 during months that did not include a normal time-series cruise (fig. 1). CalCOFI cruises are designated by year and month. CalCOFI stations are designated by line

## Multivariate ENSO Index

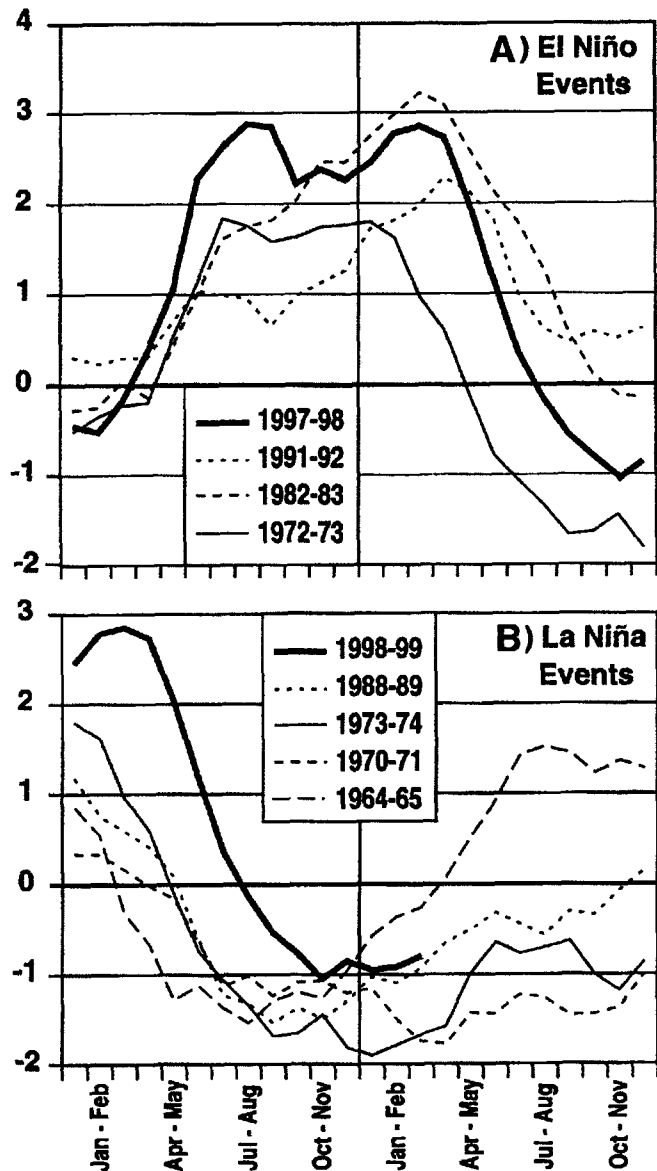


Figure 2. A monthly multivariate ENSO index, or MEI (Wolter and Timlin 1998). MEI indicates the intensity of (A) the 1997-98 El Niño relative to three recent strong El Niño events, and (B) the 1998-99 La Niña relative to four recent La Niña events.

and station number. Cruise patterns, methods, and data from the CalCOFI time-series cruises are published in data reports (Scripps Institution of Oceanography 1999), and this information is also available on the World Wide Web (<http://www-mlrq.ucsd.edu/calcofi.html>). Methods and data sources for data from other programs are briefly listed as the observations are presented.

## OBSERVATIONS

### Atmospheric Conditions

During 1998-99, many atmospheric and ocean fields in the equatorial and north Pacific, including sea-level

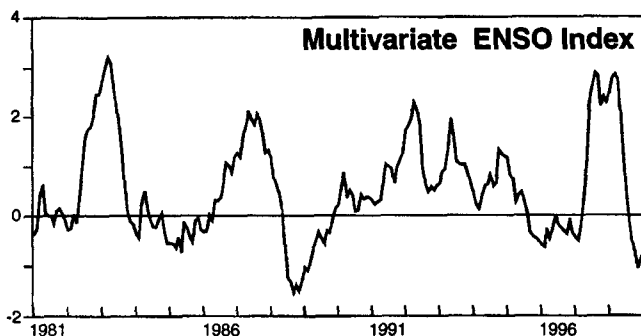


Figure 3. Monthly time series of the multivariate El Niño index, or MEI (Wolter and Timlin 1998), for 1981-98. The series highlights the rapid transition from El Niño to La Niña in 1998.

pressure (SLP), wind stress, and sea-surface temperature (SST), typified classic El Niño and La Niña patterns (cf. Murphree and Reynolds 1995). In the tropical Pacific, 1998 was marked by a dramatic transition from one of the strongest El Niño events this century to a strong La Niña event. The multivariate ENSO index (MEI; Wolter and Timlin 1998) shows this change. The MEI dropped from an El Niño peak in spring 1998 to a minimum in late fall 1998 (fig. 2). This decline was unprecedented in the nearly 50-year history of the MEI (fig. 3).

In early 1998, the 1997-98 El Niño reached a second peak in intensity (fig. 2A; the first having been in summer 1997). The event was clearly affecting the North Pacific Ocean at this time (Lynn et al. 1998). Beginning in March 1998, however, El Niño conditions in the equatorial Pacific weakened considerably (fig. 2B). Negative SST anomalies (SSTAs) developed in the central and eastern equatorial Pacific during May (NCEP 1998a). Anomalously cool subsurface (50-300 m) temperatures extended along the equator from the western Pacific well into the eastern Pacific (NCEP 1998a). This pattern resulted from the eastward expansion of a shoaling thermocline from the western Pacific beginning in July 1997 (NCEP 1997a). This suggested a clear transition toward La Niña conditions in the tropics. Anomalies of SLP (Kalnay et al. 1966) and SST (Reynolds and Smith 1995) for the Pacific illustrate the evolution of this event. SLP and Reynolds SST data were provided by the NOAA-CIRES Climate Diagnostics Center, Boulder Colo., from its Web site (<http://www.cdc.noaa.gov>).

SST anomalies were still characteristic of El Niño conditions during April-May 1998 (fig. 4B). Very warm SST anomalies (+2° to 4°C) extended west from South America along the equator. The North and South American coasts remained unseasonably warm (+1° to 2°), while the central north and south Pacific were unusually cool (-1° to -2°). Cool anomalies in the central north Pacific continued to shift east, as warm anomalies in the Kuroshio extension expanded east across the date line.

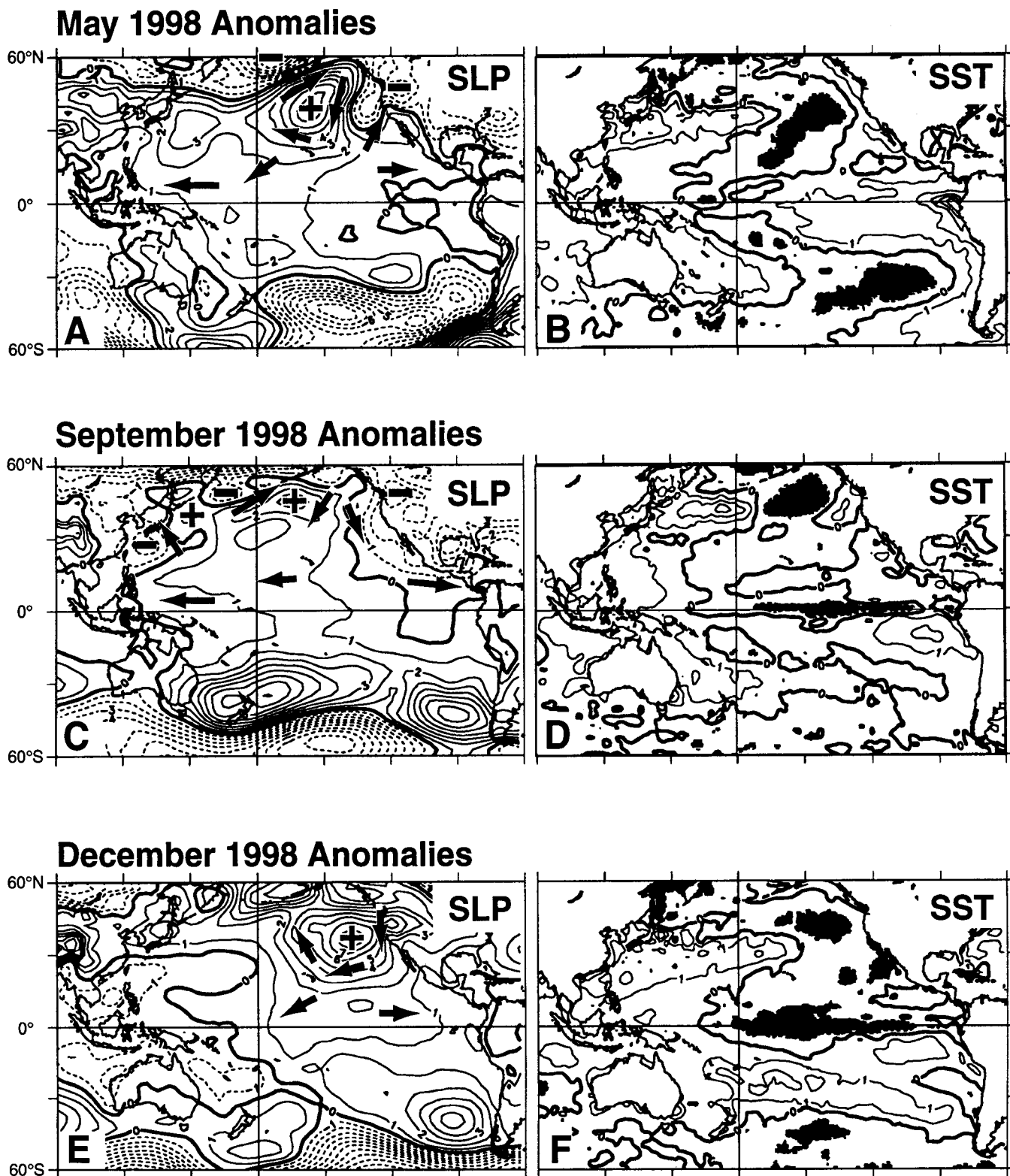


Figure 4. Anomalies over the Pacific Ocean for May, September, and December of 1998: A, C, and E, sea-level pressure (SLP) with anomalous surface wind; B, D, and F, sea-surface temperature (SST). Positive anomalies denote higher than normal atmospheric pressure and warmer than normal SST. Contour intervals are 1 mb and 1°C. Shading denotes SST anomalies greater than  $-1^{\circ}$ . Arrows indicate the direction and strength of the wind anomalies. Anomalous surface winds are approximately parallel with SLPA contours, and cyclonic (counterclockwise in Northern Hemisphere) around negative anomalies. Closer-spaced SLPA contours indicate faster anomalous winds. Monthly data were obtained from the Climate Diagnostics Center. The SLP climatology period is 1968–96; the Reynolds SST climatology period is 1950–79.

The North Pacific High (NPH) pressure system is normally unseasonably weak (strong) during El Niño (La Niña) events. The NPH intensified east of the date line during April–May 1998, leading to a positive SLP anomaly in the northeast Pacific (fig. 4A). The resulting trade winds were stronger than usual, a precursor to the developing La Niña. Anomalously strong anticyclonic atmospheric circulation contributed to greater offshore surface Ekman transport near the U.S. west coast, which favored upwelling and cooler SSTs. This atmospheric pattern is likely to produce lower coastal sea level, a shallower thermocline, and increased equatorward flow in the California Current system (CCS). The opposite can be expected during El Niño events.

By early autumn 1998, coastal SSTAs along North and South America had diminished to near normal (fig. 4D). Negative SSTAs extended across the eastern tropical Pacific to near South America. Warm anomalies intensified from Japan to the date line. By October a shift to strong southward wind stress had produced cooler than normal SSTs in the CCS.

Anomalous atmospheric wave train activity emanating from east Asia displayed a pattern of alternating positive and negative centers that arced across the North Pacific (cf. Nitta 1987), as illustrated in figure 4C. This pattern is very reminiscent of a wave train seen in the developing phase of El Niño one year previously (Lynn et al. 1998; fig. 4C), but with the signs reversed. This late summer atmospheric teleconnection pattern in 1998 seems to be responsible for anomalous surface Ekman transports and a complex pattern of positive and negative SST anomalies over the north Pacific.

Trade winds continued to be stronger than normal at this time, a characteristic of La Niña events and counter to the pattern observed during El Niño events. Equatorial wind anomalies were divergent from the central tropical Pacific, again opposite those in the 1997–98 El Niño (Lynn et al. 1998). This divergence may have been partly responsible for the cool equatorial SST anomalies. An unusually shallow thermocline along the equator east of the date line, characteristic of La Niña events, produced negative subsurface temperature anomalies of 5° to 7°C at depths of 50–150 m (NCEP 1998b). A year earlier this region featured a deeper than normal thermocline and positive temperature anomalies of this magnitude.

By late 1998, atmosphere and ocean anomaly fields displayed a classic fully developed La Niña pattern (cf. Murphree and Reynolds 1995). Higher than normal SLP covered most of the north Pacific (fig. 4E). A well-developed North Pacific High, typically dominant only in spring and summer, produced strong anticyclonic winds over the northeast Pacific. This is related to the patterns of atmospheric convection, as reflected by anomalies in outgoing longwave radiation (OLRA). During

the latter half of 1998, OLRA in the central tropical Pacific and the CCS were positive (cf. NCEP 1998c), indicating low convection in these areas. Negative OLRA and higher than normal convection were observed in the western tropical Pacific and over southeast Asia. The atmospheric flow into and out of these regions of unusual convection feeds into the upper tropospheric jets. The development and maintenance of pressure anomalies in the extratropics are teleconnected to tropical atmospheric anomalies through these jets (Murphree and Reynolds 1995).

Atmospheric flow anomalies are also responsible for redistributing heat and moisture. The unusual distribution of pressure during winter 1998–99 (fig. 4E) displaced the north Pacific jet stream northward. Winter storms favored a track over the northwest United States, bringing unseasonably heavy precipitation to Washington and Oregon, and leaving southern California relatively free of the intense storms experienced in early 1998.

Strong upwelling-favorable winds along the U.S. west coast associated with the strong NPH contributed to SSTs more than 1°C below normal (fig. 4F). SSTs up to 2° below normal stretched along much of the equator. Positive SSTAs covered the north Pacific west of the dateline.

A continuation of the La Niña patterns described above is shown in the most recent climate summaries, available for March 1999 (NCEP 1999). Equatorial and northeast Pacific SSTAs remained up to 1° to 2° below normal. High SLP over the northeast Pacific continued to generate strong upwelling-favorable wind stress along the U.S. west coast and feed into unusually intense trade winds. The MEI has remained level since late 1998 (fig. 2B). Historically, the MEI has stayed negative for many months following a La Niña event (e.g., 1970–71, 1988–89). However, conditions could shift back to El Niño as well (e.g., 1964–65). In recent months a deep thermocline in the western tropical Pacific has been developing and moving east (NCEP 1999). If this trend continues, El Niño conditions may develop later this year. Subsurface tropical temperature anomalies are reminiscent of those prior to the 1997–98 El Niño event (cf. NCEP 1997b).

### Physical Structure and Ocean Circulation

Data taken at coastal shore stations and buoys have the advantages of a higher sampling frequency, greater alongshore geographic coverage, more rapid data distribution, and, in the case of the shore stations, longer periods of measurements. A challenge for CalCOFI is to improve our ability to use these data in order to make inferences about oceanographic and ecosystem structure in the offshore waters and improve our understanding of events on time scales shorter than can be resolved by

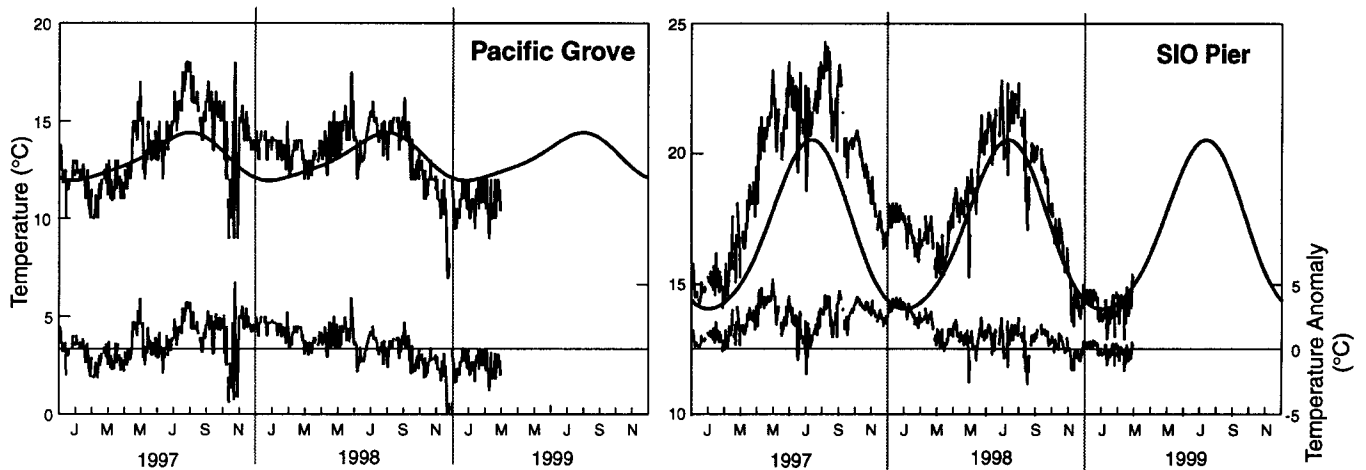


Figure 5. Sea-surface temperature at Pacific Grove and La Jolla (SIO Pier) for 1998 and 1999. Daily temperature and anomalies from the long-term harmonic mean (1919–93 for Pacific Grove and 1916–93 for La Jolla). The harmonic mean annual cycle in SST is also shown.

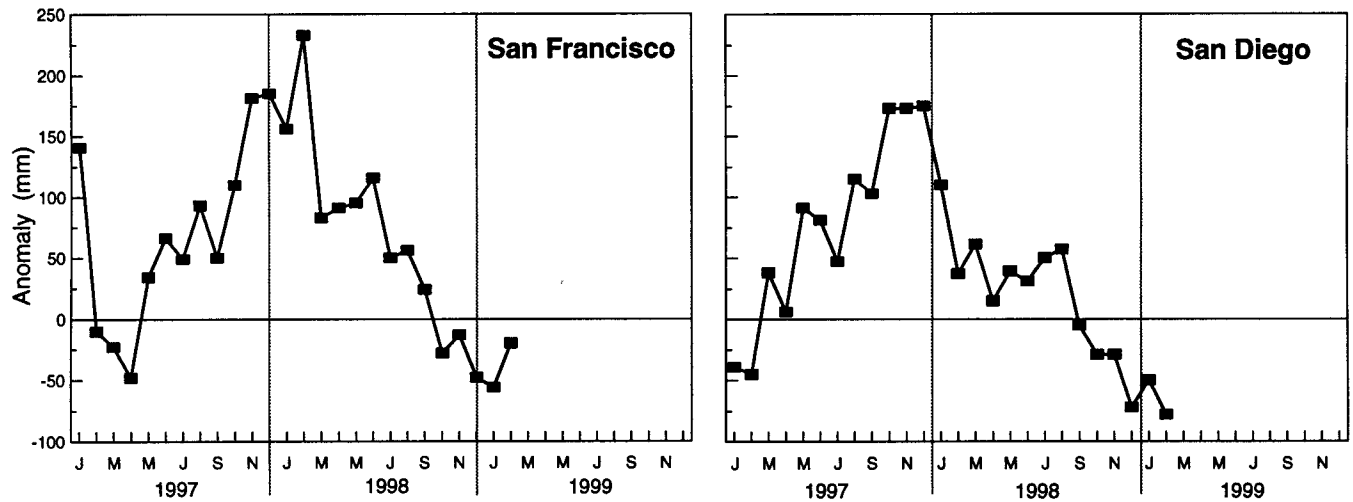


Figure 6. Monthly sea-level anomalies at San Francisco and San Diego for 1997, 1998, and 1999. The monthly anomalies are deviations from the 1975–95 period, corrected for atmospheric pressure.

the quarterly time-series cruises (McGowan et al. 1998). Since there has been a secular trend of warming and rising sea level since the mid-1970s (Roemmich 1992), it is important to consider the base period used to calculate the climatologies when comparing anomalies derived from different data sources. Coastal shore station temperature anomalies were calculated upon the base period of 1916–93 for La Jolla and 1919–93 for Pacific Grove (Walker et al. 1994). Sea-surface temperature at La Jolla was anomalously warm throughout 1997 and most of 1998, with only a few cool episodes of near-normal temperatures (fig. 5). Sea-surface temperature was normal to cool from the fall of 1998 through the early spring of 1999. Pacific Grove was cool to normal in the early part of 1997. Positive temperature anomalies were generally observed from August 1997 to September of 1998, although there were several episodes of below-normal temperatures. From October 1998

through the spring of 1999 temperatures were generally cooler than normal.

Sea-level anomalies (the difference between the mean sea level for the given month and the mean annual cycle for 1975 to 1995 corrected for the inverse barometer effect) provide another index of oceanographic structure that can be measured at coastal shore stations. San Diego and San Francisco showed quite similar temporal patterns from 1997 to early 1999 (fig. 6). Sea level began to rise to anomalously high values indicative of El Niño in May 1997, and remained anomalously high until September–October 1998. The highest values occurred from October 1997 to February 1998. Values in the fall and winter of 1998 and early 1999 were anomalously low. It may be that the similarity in the sea-level signal was due to the strong El Niño forcing standing out above the regional variability. The sea-level data were provided by the Joint Archive for Sea Level

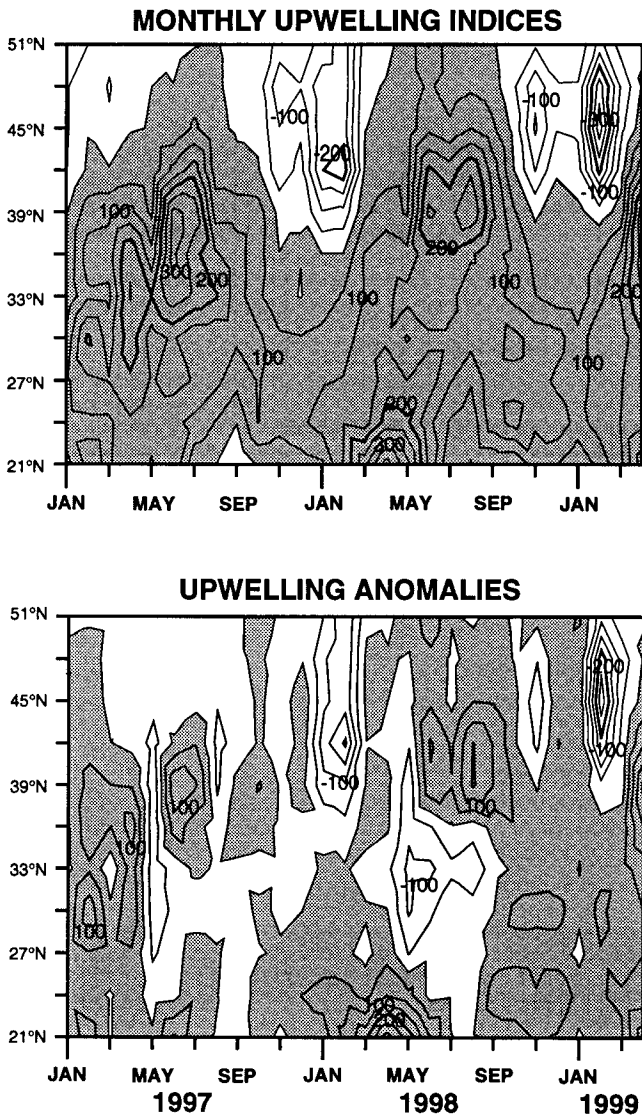


Figure 7. Monthly upwelling index and upwelling index anomaly for January 1997 to April 1999. Shaded areas denote positive (upwelling-favorable) values in the upper panel, and positive anomalies (greater than normal upwelling) in the lower panel. Anomalies are relative to the 1948–67 monthly means. Units are  $m^{-3} sec^{-1}$  per 100 km of coastline.

(JASL), a collaboration between the University of Hawaii Sea Level Center and the National Oceanographic Data Center <http://uhslc.soest.hawaii.edu/uhslc/jasl.html>.

Monthly coastal upwelling indices (Bakun 1973; Schwing et al. 1996) provide an index of atmospheric forcing of ocean circulation. The upwelling index during 1998 and early 1999 featured four periods of negative anomalies (fig. 7). Unusually strong downwelling extended north from Monterey in early 1998, and returned in November 1998 and February 1999. Weaker than normal upwelling occurred through late spring and summer 1998 from Monterey south to Baja California. Lower upwelling rates stretched along the entire west coast in May 1998. The remainder of 1998 and early 1999 featured higher than normal upwelling. Upwelling

was particularly strong off northern California in late summer, and along the entire coast in April 1999. Upwelling anomalies along California in April 1999 ( $100\text{--}200 m^{-3} s^{-1}$  per 100 km of coastline) were among the largest in the over 50-year record of the upwelling index. They were comparable to anomalies in the early spring of other La Niña years (e.g., 1964, 1968). However, not all La Niña years featured anomalously strong coastal California upwelling in spring, and years of very strong upwelling were not necessarily linked to equatorial La Niña events. SSTs in the CCS closely reflect these perturbations in coastal upwelling (fig. 4, also R. Mendelsohn, NOAA/PFEL, pers. comm.). The periods of high upwelling indices in the spring of 1999 were coincident with the decline in SST anomalies at the coastal shore stations to below normal values and the decline in sea level to below normal values. The changes in all of these indices are consistent with the transition to cool-water conditions.

Direct measurements of ocean temperature and winds at coastal buoys provide an additional source of information about physical processes that influence the California Current ecosystem. National Data Buoy Center winds at selected available locations along the U.S. west coast (fig. 8) display the short-term variability associated with synoptic atmospheric events which were superimposed on the annual climatological cycle of strong southward wind in summer and northward or weak southward wind in winter. Wind vectors align strongly with the local coastline (table 1). Returns of buoy data have been spotty over much of the past few years.

The 1997–98 winter featured numerous episodes of greater than normal northward buoy winds (more downwelling-favorable), and generally highly variable wind speeds. These were associated with heavy winter storm activity and copious precipitation for much of the Pacific Northwest. Winter winds were very strong and oscillated in direction even in the Southern California Bight, where winds are normally relatively weak and variable (cf. 1997). In late 1998, anomalous northward winds off northern California and Oregon were followed by a period of very strong southward winds. The upwelling index anomalies (fig. 4) correspond well with the tendencies of the buoy alongshore winds, with both indicating anomalous downwelling in early 1998, and greater than normal upwelling in the latter half of 1998.

From a peak in August–September 1997, when temperatures were as much as  $6^{\circ}C$  above average, buoy SSTs gradually cooled and returned to their climatological values by spring 1998 (fig. 9). SSTs remained near normal through most of 1998, fluctuating on synoptic (10–30 day) time scales in response to changing wind patterns. In late 1998, SSTs dropped to well below nor-

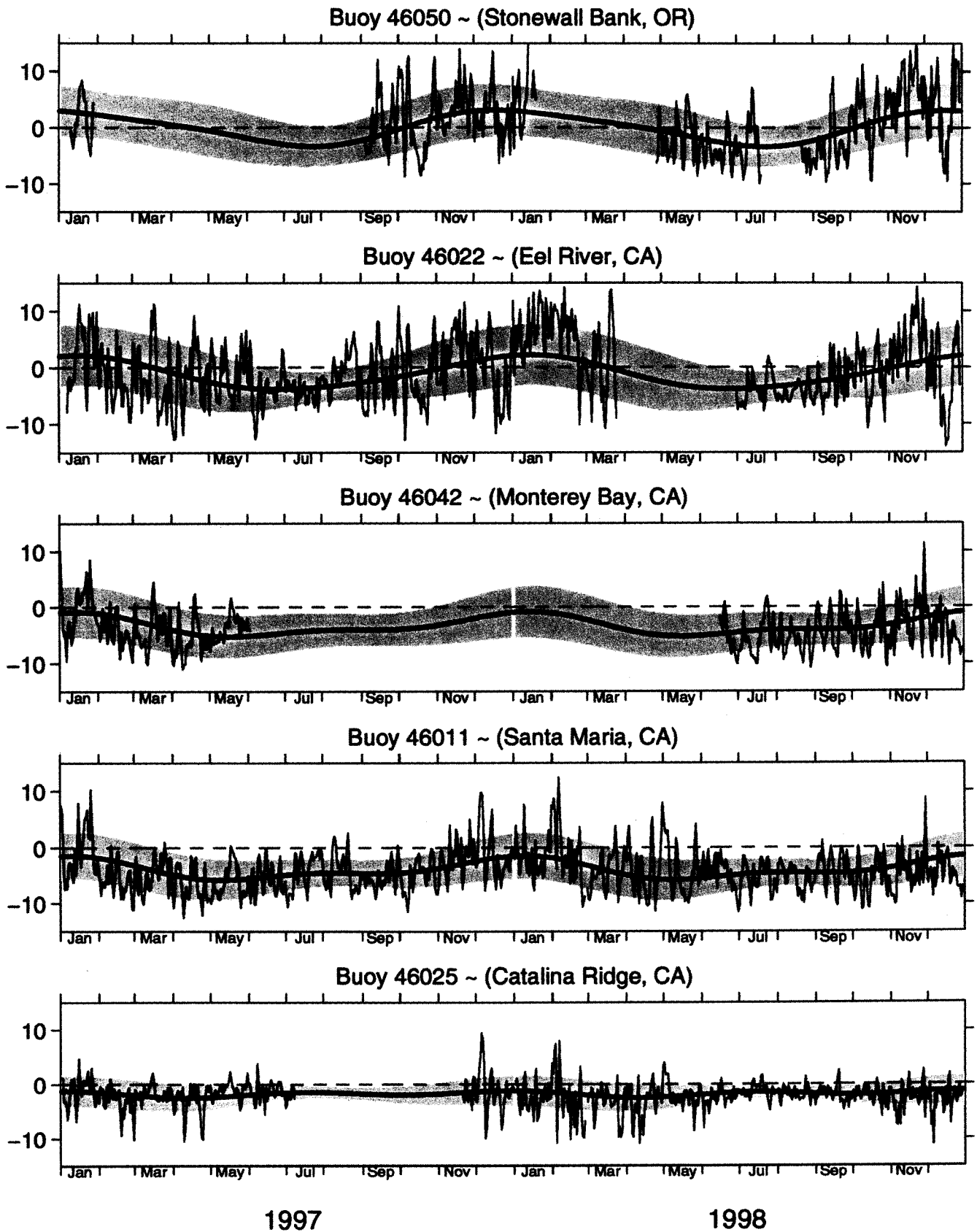


Figure 8. Time series of daily-averaged alongshore winds (knots) for 1997-98 at selected NDBC buoys. Bold lines are the harmonic mean annual cycle at each buoy. Shaded areas are the standard error for each Julian day. The period used for calculating the mean at each site and the alongshore angle are shown in table 1.

TABLE 1  
 Locations of SST and Alongshore Wind Time Series

Buoy	Name	Position	Base Period <sup>a</sup>	Alongshore angle (°N) <sup>b</sup>
46050	Stonewall Bank, Ore.	44.6°N 124.5°W	1991–98	0
46022	Eel River, Calif.	40.8°N 124.5°W	1982–98	354
46042	Monterey Bay, Calif.	36.7°N 122.4°W	1987–98	328
46011	Santa Maria, Calif.	34.9°N 120.9°W	1980–98	326
46025	Catalina Ridge, Calif.	33.7°N 119.1°W	1982–98	294

<sup>a</sup>Period of harmonic mean.

<sup>b</sup>Determined from principal-component analysis.

mal in response to a period of very strong equatorward (upwelling-favorable) wind stress.

Atmospheric changes presumably contribute to variations in upper ocean temperature through changes in upwelling and downwelling rates, turbulent mixing and stratification, and air-sea heat exchange. However, not all wind events produce an obvious response in SST. Synoptic changes in SST were unusually light during November 1997–April 1998, despite vigorous wind variability on this scale. The steady decline in SST over this period suggests an unusually deep mixed layer. Even during episodes of strong equatorward wind, surface water may have been replaced by upwelled water of virtually the same temperature.

The oceanographic and biological data from the CalCOFI time-series cruises provide additional information about subsurface patterns and ecosystem structure. Patterns in these data can be considered in the context of the long-term mean circulation patterns (fig. 10). Since many studies have shown strong associations between ecosystem structure and circulation patterns in the California Current region (Hayward and Mantyla 1990; Strub et al. 1991; Haury et al. 1993; Hayward and Venrick 1998), the mean circulation pattern is a useful reference for physical structure. The location of the low-salinity jet which forms the core of the California Current, the continuity and strength of the coastal countercurrent, as well as the location and strength of mesoscale features including coastal filaments, eddies, and meanders of the California Current are associated with changes in plankton distributions and fish spawning.

Although cruise 9802 was reviewed in last year's report, we include it here because it sets the stage for the remarkable change in circulation and ecosystem structure which took place in early 1998. This cruise showed a circulation pattern consistent with strong El Niño conditions (fig. 11). There was a strong coastal countercurrent, and the low-salinity jet of the core of the California Current was unusually far offshore. Note the quite low salinity water (less than 33.0) in the core of the California Current jet in the central part of the pattern. The presence of this very low salinity water im-

plies that there was both a strong coastal countercurrent and strong southward flow of the California Current jet at this time. Surface chlorophyll was relatively low throughout the pattern, as is typical of the January–February time period.

A remarkable change in the circulation pattern and chlorophyll distribution were evident by April in the data from cruise 9804 (fig. 12). The low-salinity jet of the California Current moved inshore, close to shore. Note that this cruise sampled three additional lines to Monterey north of the normal pattern in order to better resolve the range of sardine spawning. The strong coastal countercurrent seen in February was absent. The surface chlorophyll concentration was quite high in the coastal region bounded by the inshore edge of the low-salinity jet. This enrichment was likely caused by isopycnal shoaling (Hayward and Venrick 1998). The circulation changed from quite anomalous conditions in January to a pattern that looked more similar to the climatology in April. Hydrographic data from the March mini El Niño cruise (not shown) suggest that the replacement of the coastal countercurrent with strong southward flow and the increase in chlorophyll took place between the end of January and the middle of March.

There were again strong changes in the circulation pattern between April and July 1998. The strong coastal countercurrent had returned by cruise 9807 (fig. 13). There was also strong flow of the California Current in the middle of the grid. The pattern of flow was similar to the climatology, and it is interesting in that both the California Current and the countercurrent showed strong flow. The flow field is similar to that seen in previous strong El Niño summers in the southern California region. The water in the core of the California Current is again very low in salinity (less than 33.0) even off southern California. The strong eddy located south of Point Conception also shows up in the long-term mean circulation pattern (fig. 10). Chlorophyll was high (greater than  $2 \mu\text{g l}^{-1}$ ) in the Point Conception region and in a tongue located in the region of shear between the California Current and the countercurrent off southern California.

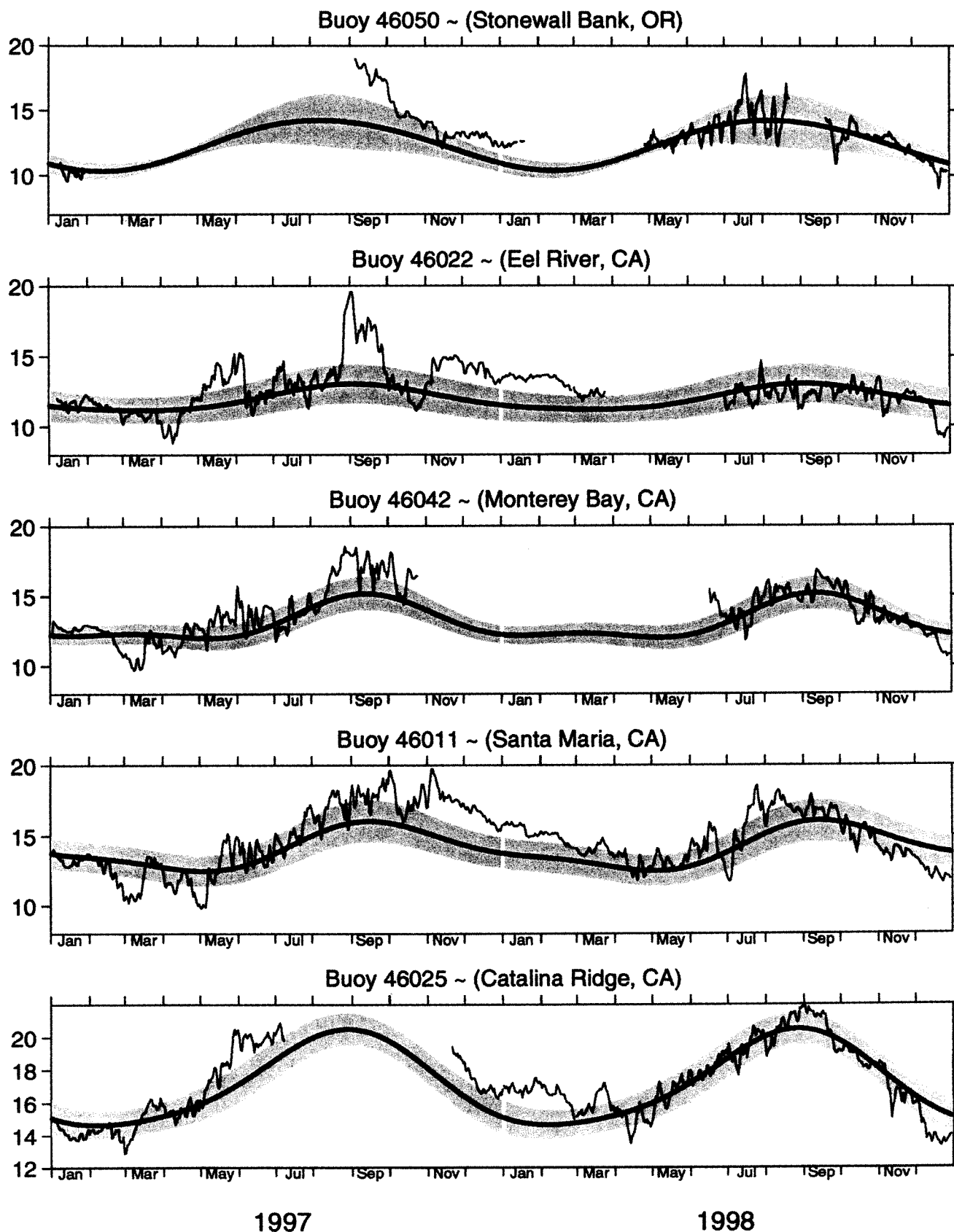


Figure 9. Time series of daily-averaged SST ( $^{\circ}\text{C}$ ) for 1997-98 at selected NDBC buoys. Bold lines are the harmonic mean annual cycle at each buoy. Shaded areas are the standard error for each Julian day. The period used for calculating the mean at each site is shown in table 1.

# LONG-TERM MEAN CIRCULATION PATTERN

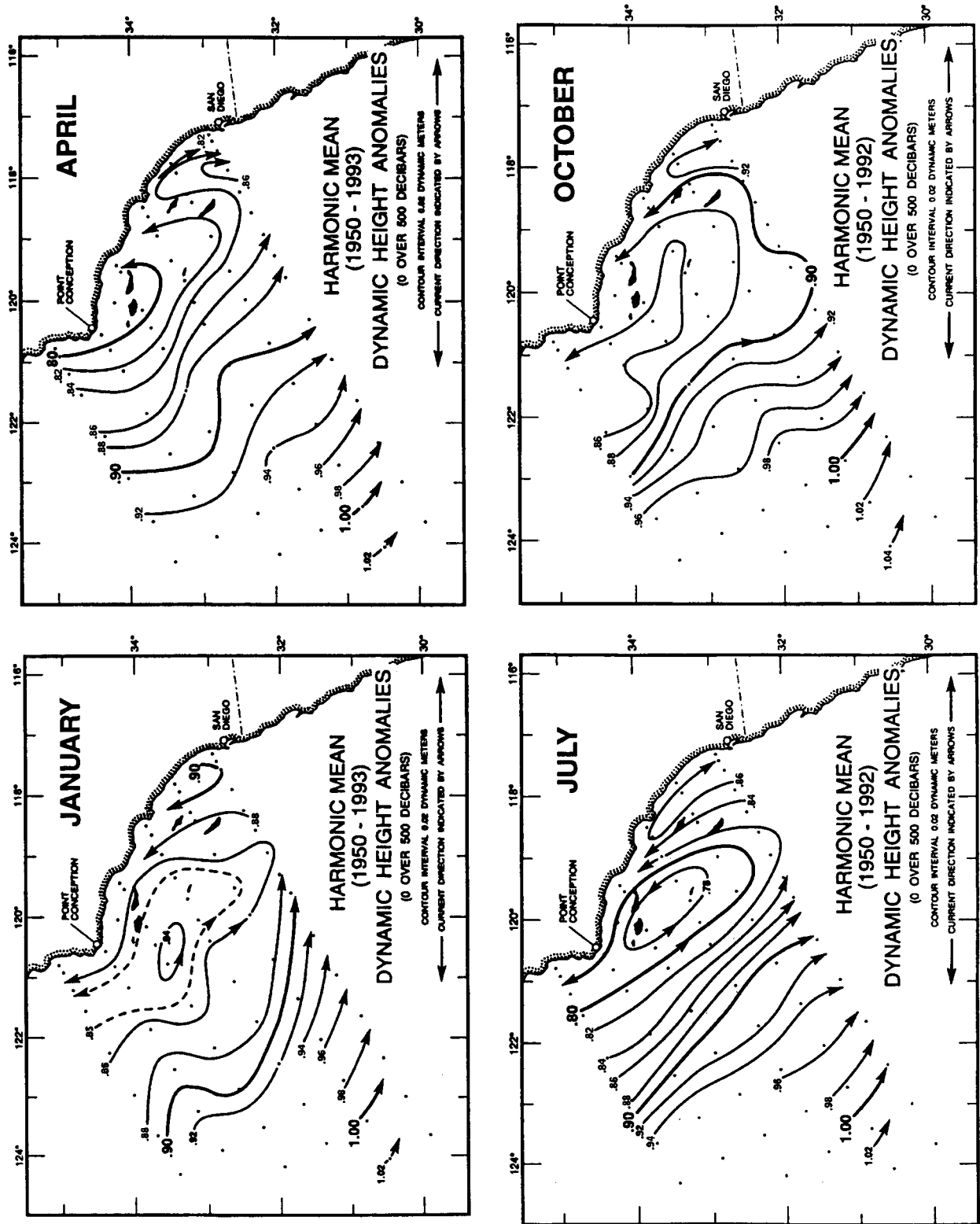


Figure 10. Long-term mean (1950-92) circulation patterns based upon 0 over 500 m dynamic height for the target months of the time-series cruises.

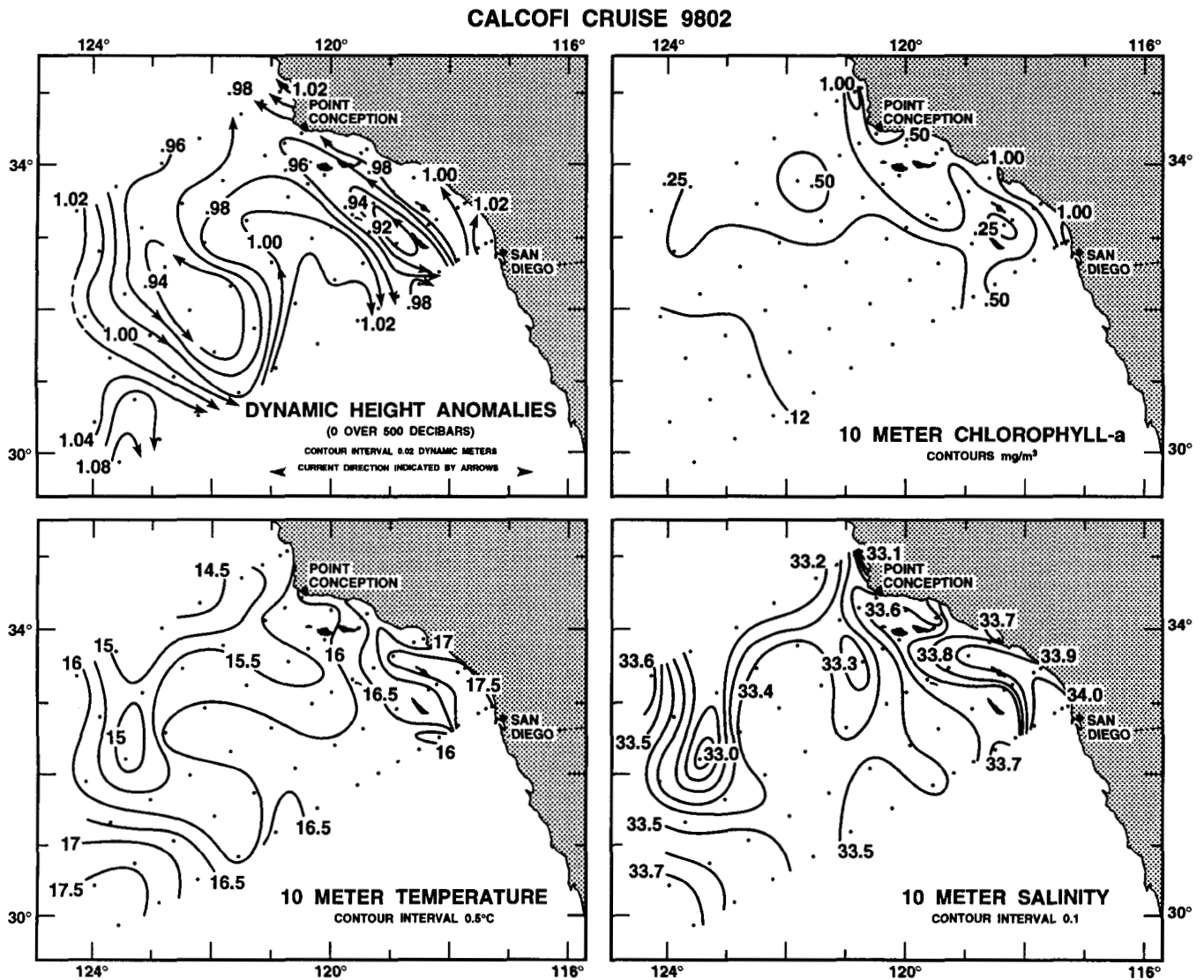


Figure 11. Spatial patterns for CalCOFI cruise 9802 (23 January–14 February 1998), including upper-ocean geostrophic flow estimated from 0 over 500 db dynamic height anomalies, 10 m chlorophyll, 10 m temperature, and 10 m salinity.

The circulation pattern on cruise 9809 (fig. 14) was again typical of the climatology, with the California Current flowing southward through the middle of the pattern, and weak northward flow along the coast. The salinity in the core of the California Current (33.1–33.2) was greater than in July. Chlorophyll was relatively low throughout the pattern, with the highest values along the coast, as is typical for fall.

The circulation pattern on cruise 9901 showed strong meandering flow of the California Current and a strong coastal countercurrent (fig. 15). The circulation pattern was strongly influenced by mesoscale structure. There were two strong mesoscale eddies and a sharp meander to the California Current. The mesoscale circulation pattern was reflected in the chlorophyll distribution. Chlorophyll was high on this cruise. Chlorophyll was elevated in an offshore tongue at the boundary between the south-

ward flow of the California Current and the northward flow of the countercurrent, and also in coastal patches. This cruise was made on RV *Roger Revelle*, and the ship's greater capability, together with a few added days of station time, allowed an expanded group of cooperative research programs, including sampling with MOCNESS.

Cruise 9904 (preliminary data) was marked by a strong mesoscale circulation pattern (fig. 16). The California Current was well offshore, and the southward extent of the penetration of water below salinity of 33.0 is consistent with strong flow. Chlorophyll was high on this cruise. Again, the spatial pattern was strongly influenced by the circulation. High chlorophyll was found at the inner edge of the low-salinity jet of the core of the California Current (Hayward and Venrick 1998).

The data collected on the monthly *Robert Gordon Sproul* mini El Niño cruises provide additional infor-

CALCOFI CRUISE 9804

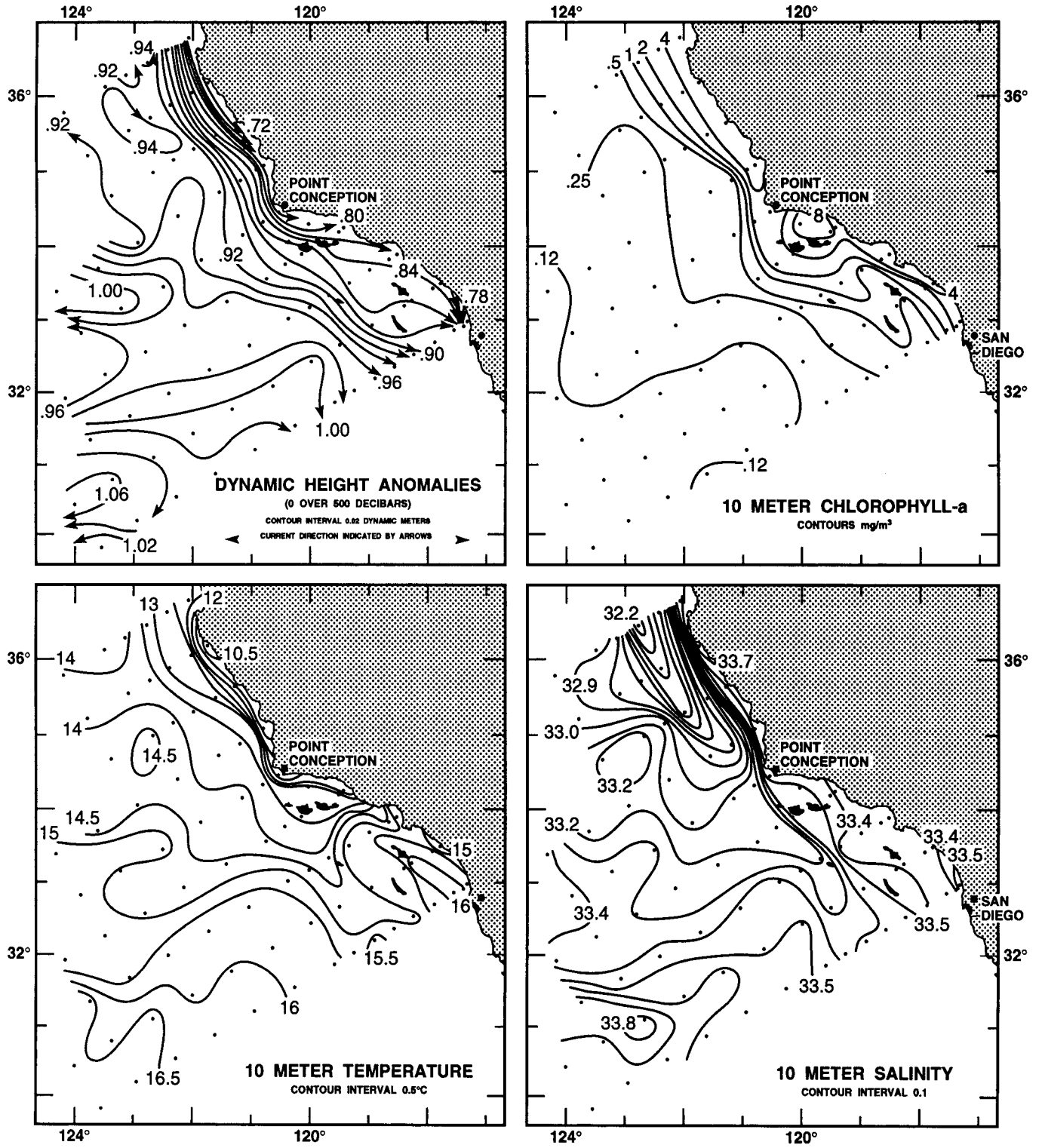


Figure 12. Spatial patterns for CalCOFI cruise 9804 (2-23 April 1998), including upper-ocean geostrophic flow estimated from 0 over 500 db dynamic height anomalies, 10 m chlorophyll, 10 m temperature, and 10 m salinity.

**CALCOFI CRUISE 9807**

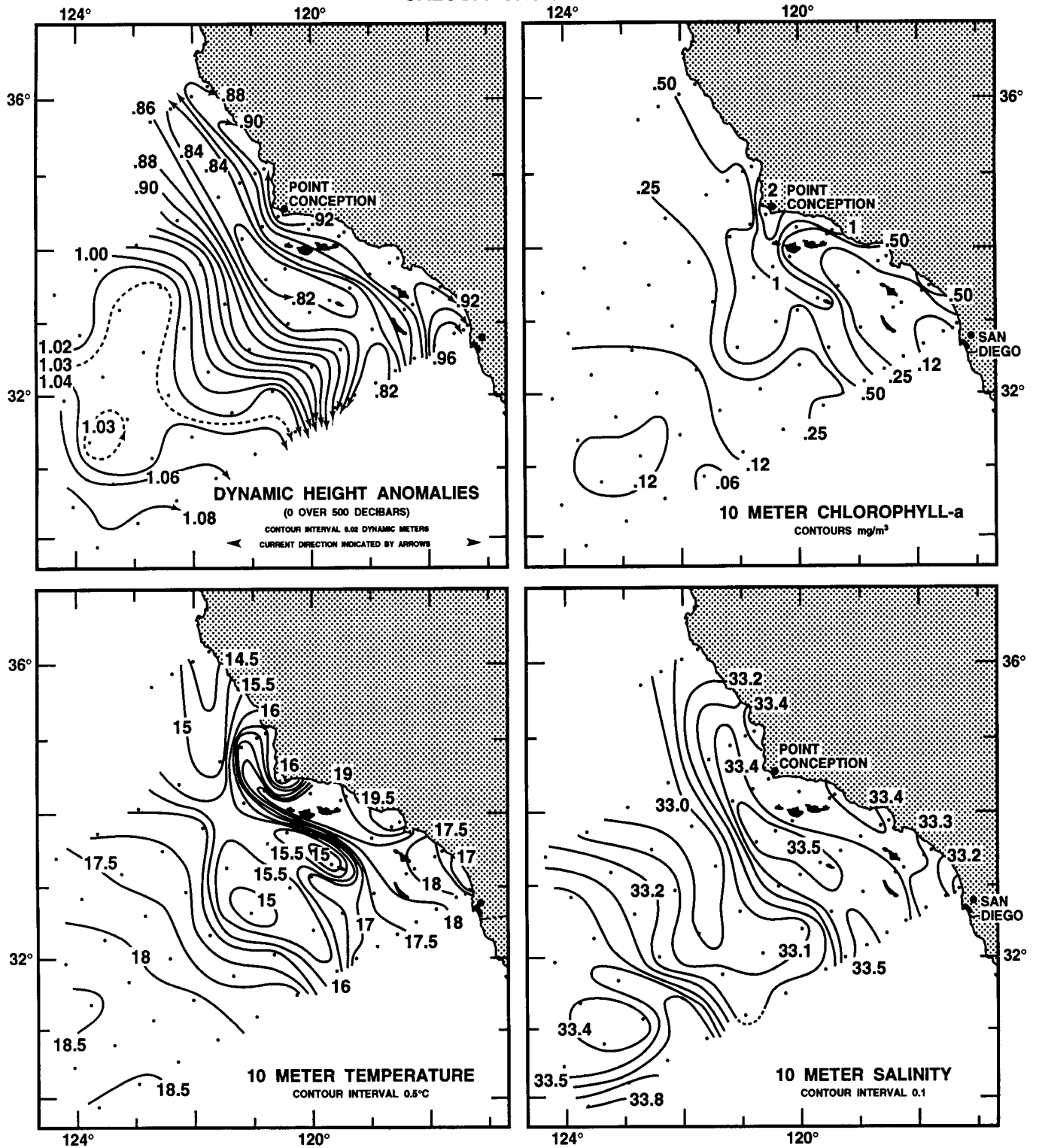


Figure 13. Spatial patterns for CalCOFI cruise 9807 (9-27 July 1998), including upper-ocean geostrophic flow estimated from 0 over 500 db dynamic height anomalies, 10 m chlorophyll, 10 m temperature, and 10 m salinity.

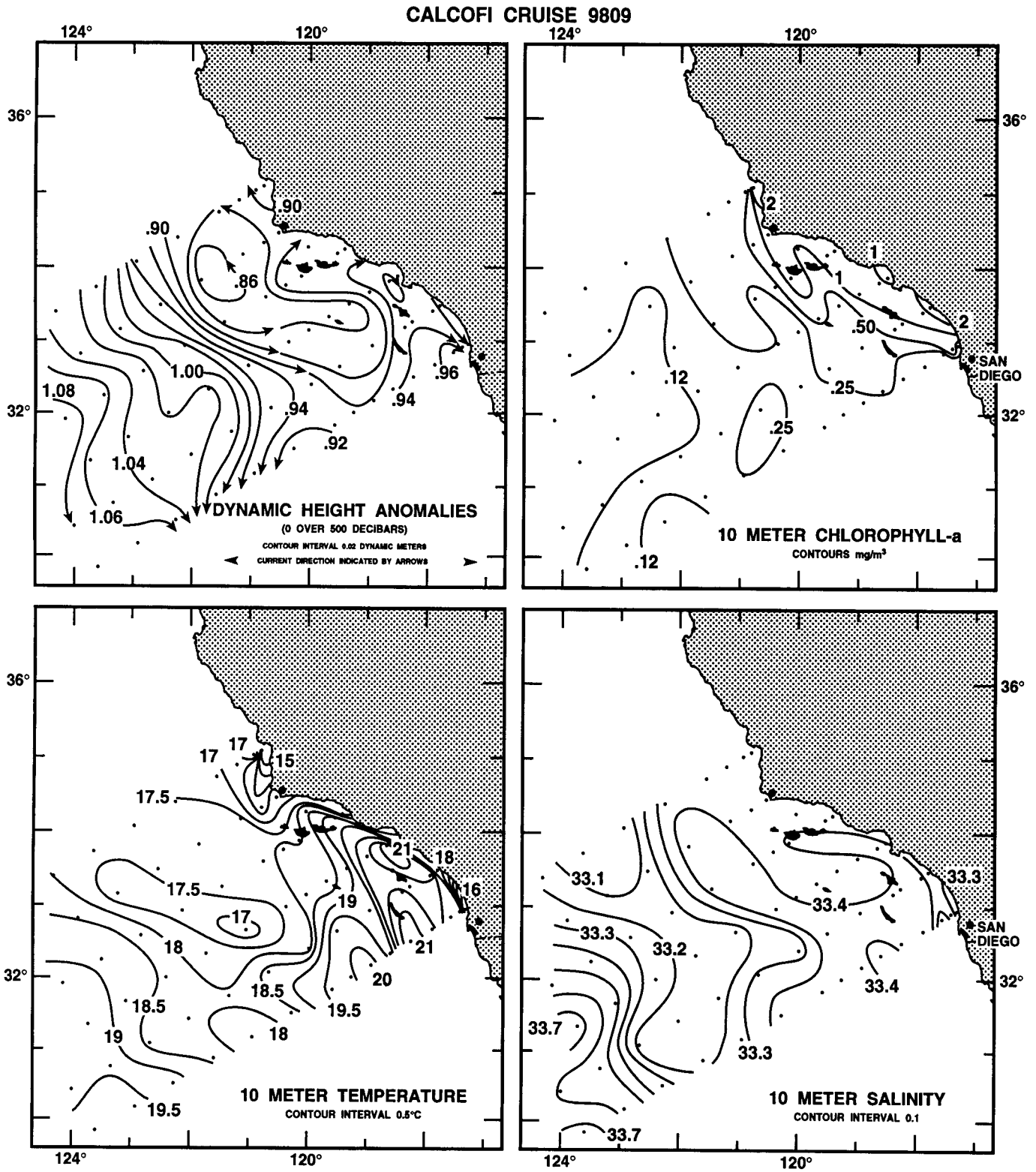


Figure 14. Spatial patterns for CalCOFI cruise 9809 (13 September–1 October 1998), including upper-ocean geostrophic flow estimated from 0 over 500 db dynamic height anomalies, 10 m chlorophyll, 10 m temperature, and 10 m salinity.

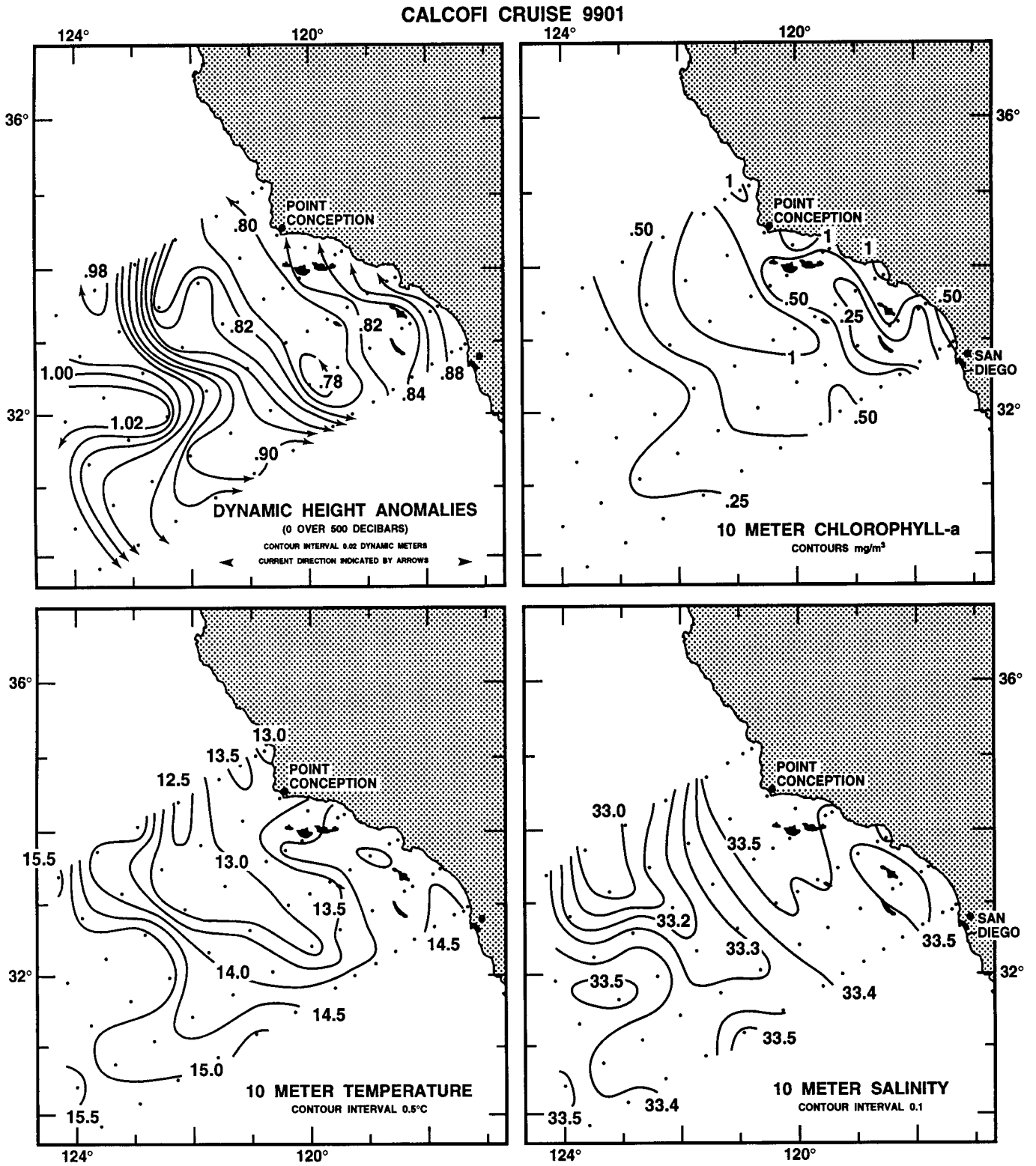


Figure 15. Spatial patterns for CalCOFI cruise 9901 (9-29 January 1999), including upper-ocean geostrophic flow estimated from 0 over 500 db dynamic height anomalies, 10 m chlorophyll, 10 m temperature, and 10 m salinity.

CALCOFI CRUISE 9904

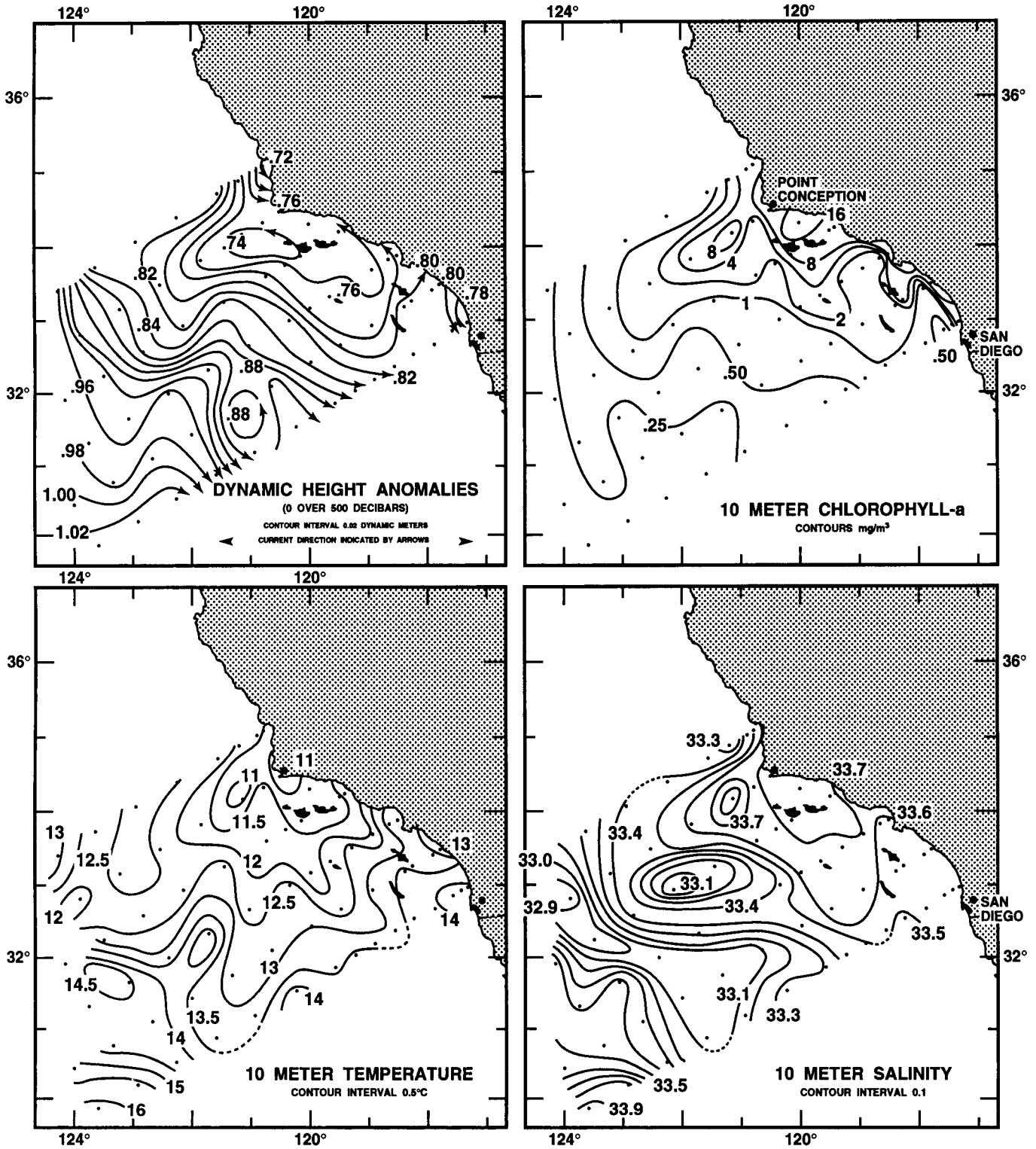


Figure 16. Spatial patterns for CalCOFI cruise 9904 (1-20 April 1999), including upper-ocean geostrophic flow estimated from 0 over 500 db dynamic height anomalies, 10 m chlorophyll, 10 m temperature, and 10 m salinity.

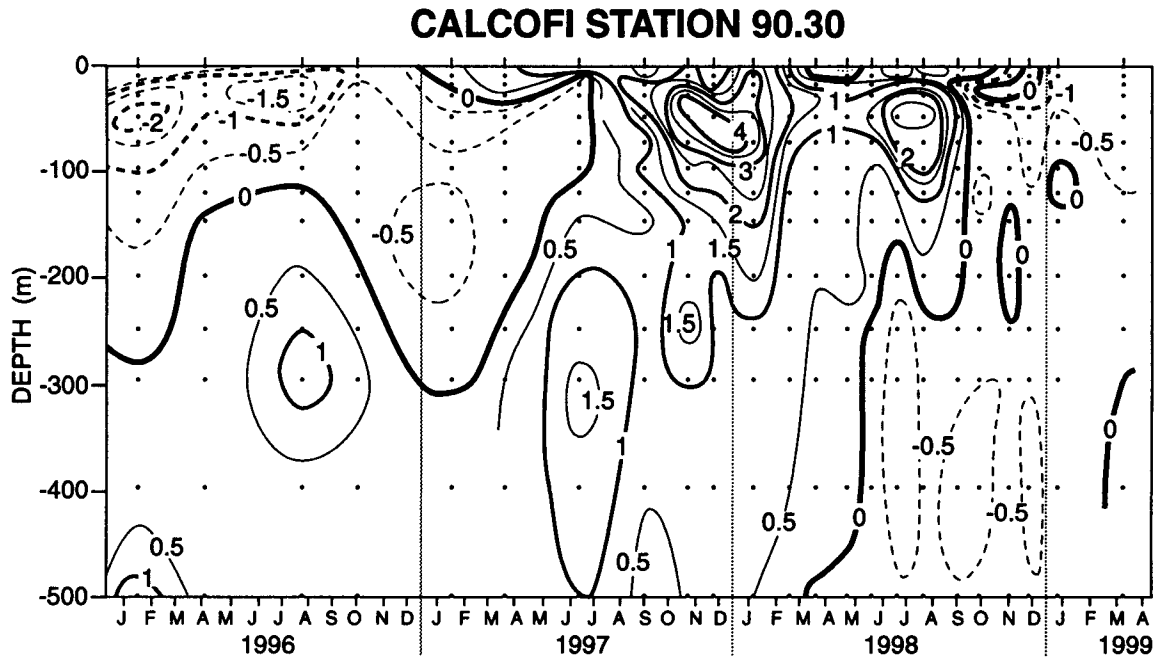


Figure 17. Anomalies in temperature ( $^{\circ}\text{C}$  from the 1950–92 base period) versus depth and time for CalCOFI station 90.30.

mation about temporal changes in structure. The analysis here focuses on pattern in upper ocean thermal structure. Vertical sections of temperature anomalies versus time are shown from stations 90.30 and 90.60 (figs. 17 and 18). Station 90.30 is located in the coastal waters influenced by the countercurrent, and station 90.60 is farther offshore in a region which is often influenced by the low-salinity jet of the California Current (fig. 1). Both stations show similar patterns of anomalies in thermal structure. At station 90.30 the surface waters showed positive temperature anomalies of greater than  $1^{\circ}\text{C}$  in July of 1997 (fig. 17). However, the waters normally found in the thermocline (50–150 m) had nearly normal temperatures. The pattern of warming increased in the fall. There was an abrupt transition to strong El Niño conditions in November 1997. This can be seen from the pattern of large (greater than  $4^{\circ}$ ) temperature anomalies in the upper thermocline. The surface waters were generally between  $1^{\circ}$  and  $2^{\circ}$  above normal throughout this period. The pattern of vertical maximum temperature anomalies in the thermocline is a characteristic structure during El Niño events in the California Current region (McGowan 1985; Lynn et al. 1995). The thermocline temperature anomalies decreased in magnitude during the spring of 1998, and there was another increase to values greater than  $2.5^{\circ}$  in July and August. The winter of 1998 and spring of 1999 were marked by cooler than normal temperatures in the upper layer. The patterns at 90.60 were quite similar to those at 90.30 (fig. 18). Again, surface temperature anomalies of greater than  $1^{\circ}$  were seen by July 1997, but temperatures in

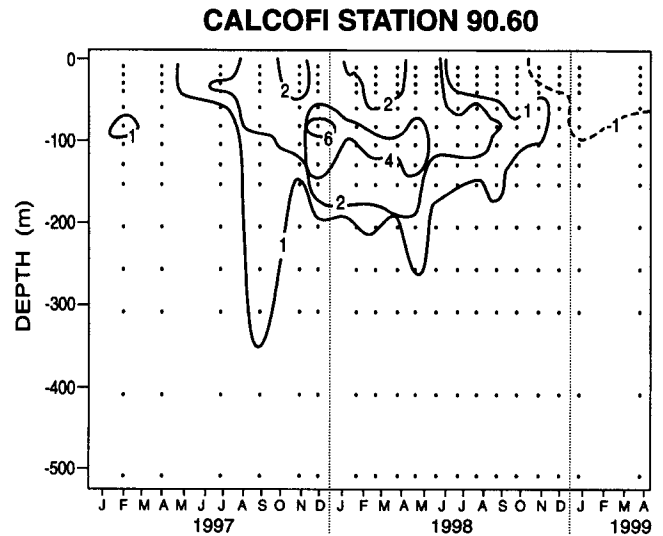


Figure 18. Anomalies in temperature ( $^{\circ}\text{C}$  from the 1950–92 base period) versus depth and time for CalCOFI station 90.60.

the thermocline were near normal. There was an abrupt shift to thermocline anomalies of greater than  $6^{\circ}$  in December 1997, and the strong thermocline anomalies persisted until September 1998. As at station 90.30, both the transition to warm and later cool temperature anomalies began at the surface and progressed downward in depth. The monthly measurements on the mini El Niño cruises show how rapidly physical structure can change in this region.

The vertical sections of temperature anomalies versus time also show that the timing of events inferred from

the thermocline signal differs from the surface signal. In November 1998 the surface waters were slightly cooler than normal, but the positive thermocline was much larger than that seen in July 1997. The patterns in anomalies derived from shore station temperature or sea level or from hydrographic data are all indices of a range of changes associated with El Niño. At any station the temperature anomalies will be influenced by both the heat content of the upper ocean and by the temperature-salinity structure. Temperature anomalies in the coastal waters will be influenced by whether cool and fresh California Current water or warm, saline water from the south is present. There is much more to be said about these data in the context of El Niño and the transition to La Niña conditions and also in the context of longer-term trends. But we have decided to not include an extensive discussion of these issues in this report because the data are still being processed and analyzed and because these events are the subject of the symposium at the 1999 CalCOFI conference. These issues will be separately presented in other publications.

Data collected to the south and north of the CalCOFI study area provide a valuable regional context. These data also will provide a basis for better defining how advection influences the abundance and species composition of the plankton. Sampling to the south was conducted by the IMECOCAL program. This program was initiated in October 1997 by seven Mexican institutions, and it has continued during 1998 and 1999. Three cruises were conducted in 1998 (January, July, and September–October; hereafter called IMECOCAL cruises 9801, 9807, and 9809) and another in January 1999 (9901). The cruises were planned to coincide closely with the timing of CalCOFI cruises off California. All cruises were made on the *Francisco de Ulloa*, and covered most of the station plan shown in figure 19. Core samples included CTD/rosette casts to 2,000 m with 5 l Niskin water samples from the surface to 150 m at standard depths. Water samples were analyzed for dissolved oxygen, inorganic nutrients, and chlorophyll. Continuous underway sampling of surface temperature and salinity, as well as continuous ADCP profiling was carried out. At each station, standard oblique bongo tows were made with 0.505 mm mesh, with one cod end dedicated to ichthyoplankton and the other to macrozooplankton. In situ productivity casts were carried out at selected stations. Cruise 9901 also included vertical CalVET tows to study fish larvae. Here we present some preliminary results based on CTD observations and dissolved oxygen measurements.

IMECOCAL cruise 9801 showed relatively weak spatial patterns (fig. 20). There was a north-south gradient in salinity, with fresher water moving into the pattern in the northwest corner in a region of weak onshore flow.

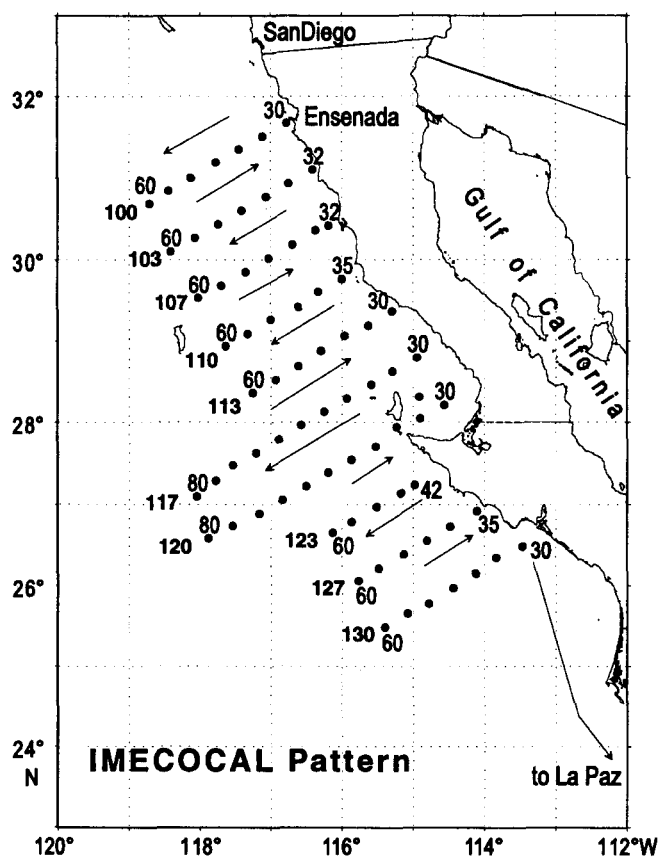


Figure 19. The IMECOCAL basic station plan.

The weak horizontal gradients in dynamic height indicate a weak circulation pattern in the study region.

Property contours depict a meandering of the California Current in July 1998 on IMECOCAL cruise 9807 (fig. 21). The flow of the California Current and a series of eddies are more clearly defined in the pattern of dynamic height. In the north, about 300 km offshore, the California Current flows east of Guadalupe Island toward Vizcaíno Bay. The current turns to the southwest when close to the coast and goes around a clockwise eddy southeast of the island. Finally, the California Current bends again southeast and returns close to the coast at the southern edge of the survey area. Poleward flows at this depth are observed south of Ensenada where the California Current splits into two branches, one flowing to the southeast and the other to the north. A coastal poleward flow trapped into a cyclonic eddy southwest of Punta Eugenia apparently does not flow north of 28°N, but bends and leaves the survey area towards the southwest. The relatively low temperatures (<17°C) and low dissolved oxygen (<5.4 ml l<sup>-1</sup>) in the region close to the coast, from 31° to 29°N, suggest the effect of coastal upwelling on this cruise.

A similar meandering flow of the California Current jet was seen on IMECOCAL cruise 9809 (fig. 22). The

### IMECOCAL Cruise 9801

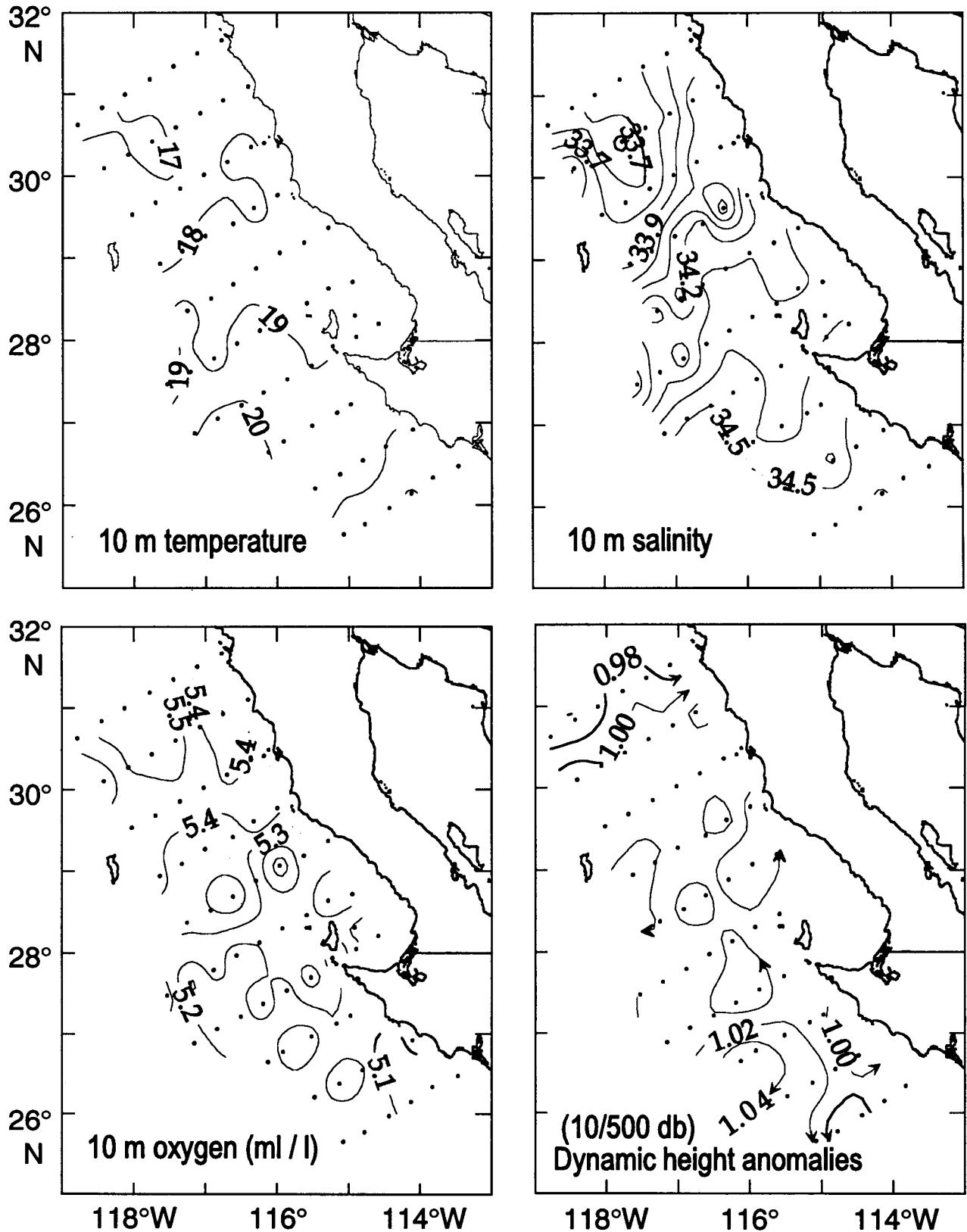


Figure 20. Spatial patterns for IMECOCAL cruise 9801 (25 January–12 February 1998) including temperature, salinity, and dissolved oxygen concentration at 10 m and geostrophic flow estimated from 0 over 500 db dynamic height anomalies.



### IMECOCAL Cruise 9809

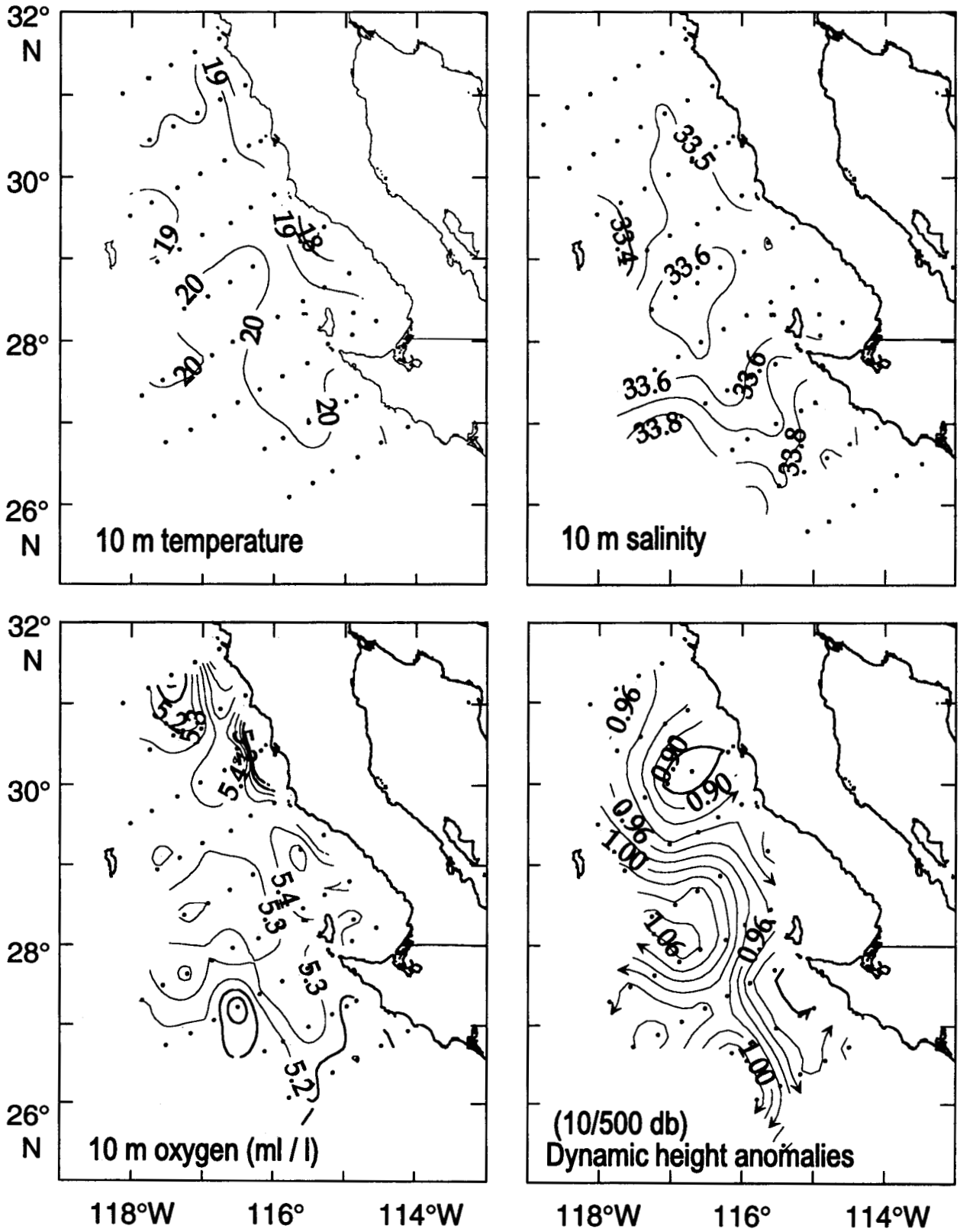


Figure 22. Spatial patterns for IMECOCAL cruise 9809 (29 September-1 October and 19 October-5 November 1998) including temperature, salinity, and dissolved oxygen concentration at 10 m and geostrophic flow estimated from 0 over 500 db dynamic height anomalies.

### IMECOCAL Cruise 9901

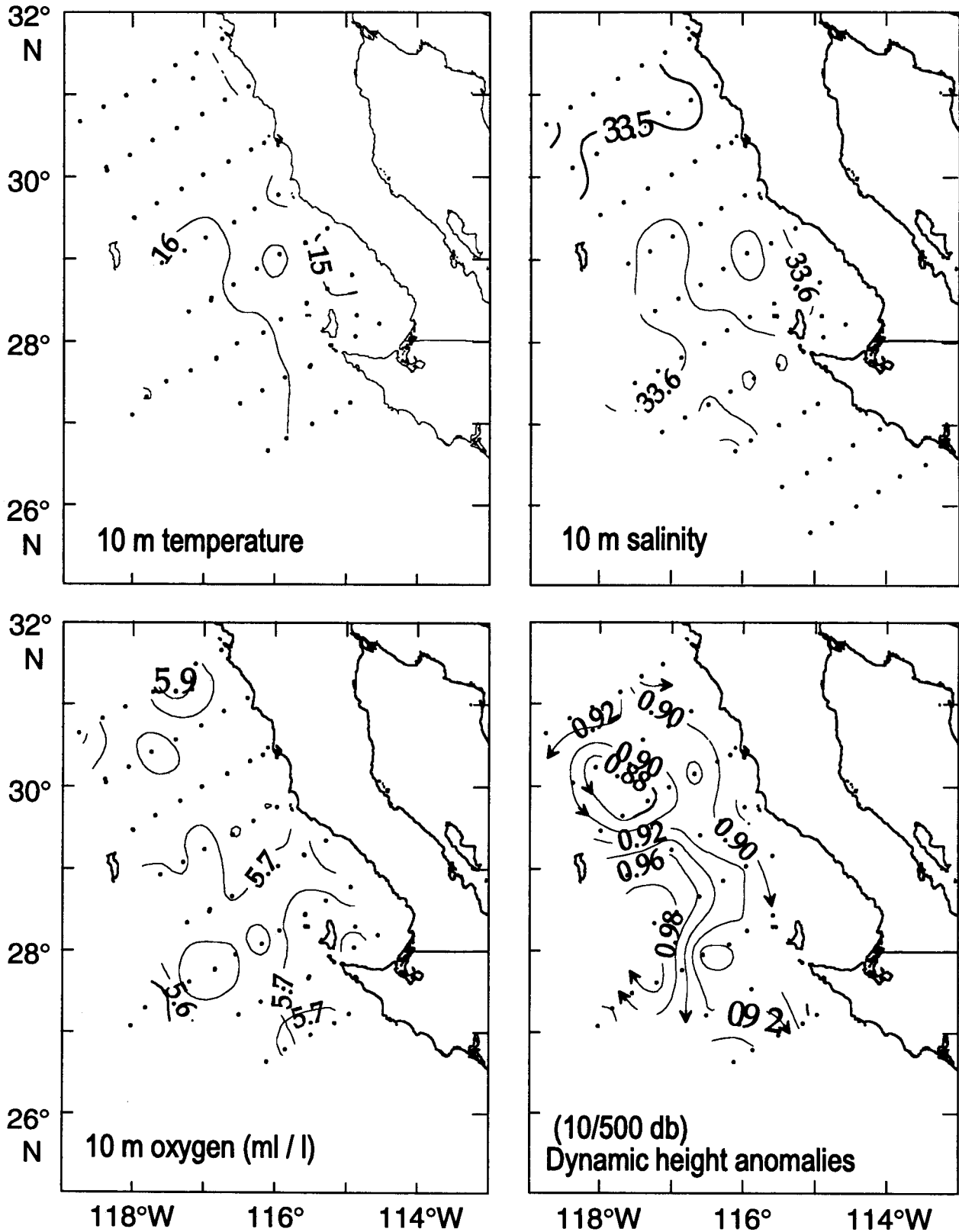


Figure 23. Spatial patterns for IMECOAL cruise 9901 (16 January–4 February 1999) including temperature, salinity, and dissolved oxygen concentration at 10 m and geostrophic flow estimated from 0 over 500 db dynamic height anomalies.

### Temperature Anomalies Line 120

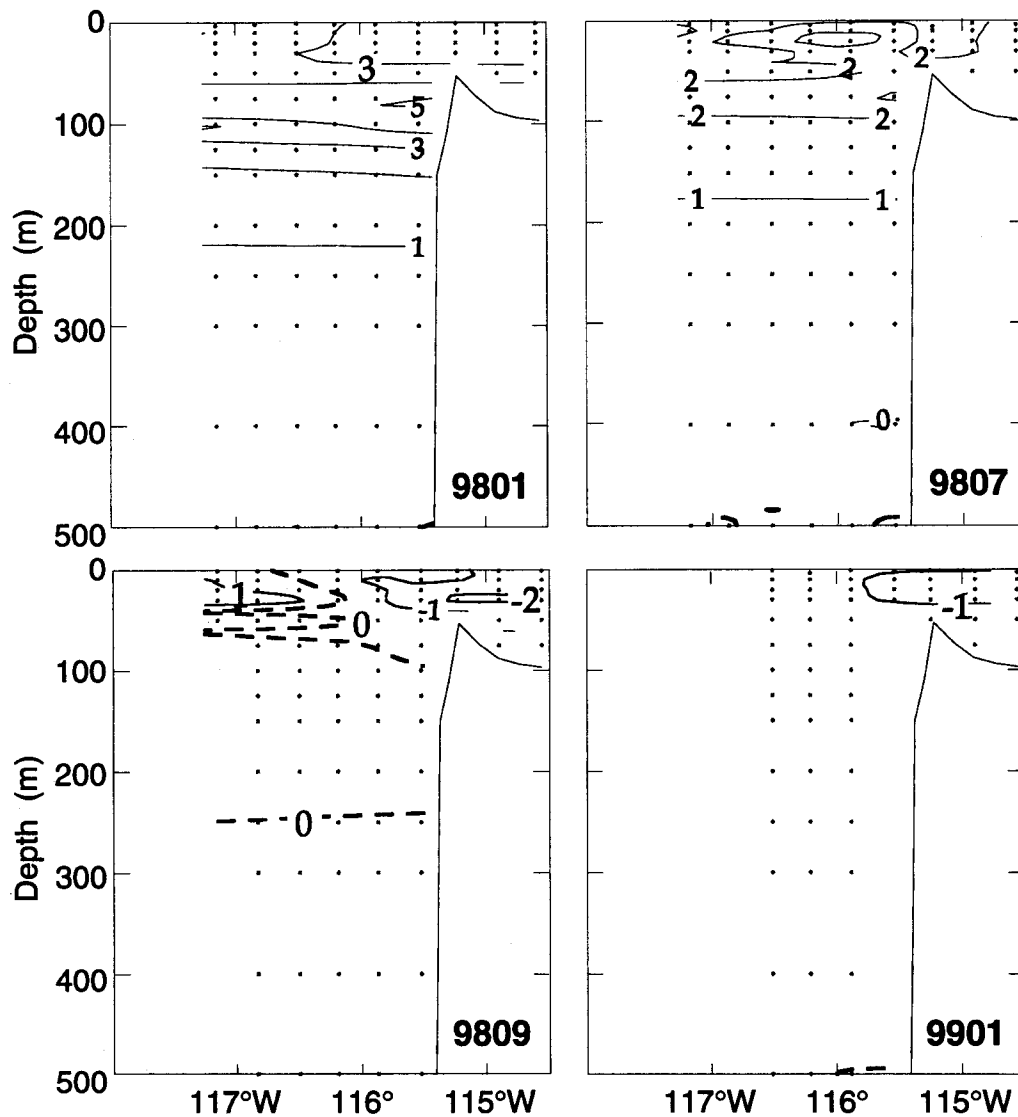


Figure 24. Temperature anomalies ( $^{\circ}\text{C}$ ) for line 120 from IMECOCAL cruises 9801, 9807, 9809, and 9901. Anomalies were calculated from mean values given by Lynn et al. (1982) for the period 1950–78.

California Current enters the region with a flow predominantly south, moves shoreward, and then southward around the clockwise meander near Guadalupe Island and leaves the area apparently in three branches—to the west, south, and shoreward. Coastal poleward flows are observed off San Quintín ( $30^{\circ}\text{N}$ ) and off Punta Eugenia ( $27^{\circ}\text{N}$ ). From  $31^{\circ}$  to  $28^{\circ}\text{N}$ , low temperatures nearshore ( $<18^{\circ}$ ) associated with low dissolved oxygen ( $<5\text{ ml l}^{-1}$ ) indicate coastal upwelling.

There was a relatively homogeneous distribution of nearsurface properties on IMECOCAL cruise 9901 (fig. 23). Lower temperatures ( $<15^{\circ}\text{C}$ ) are found off capes and north of Vizcaíno Bay. During this cruise, strong and persistent northwesterly winds were observed. The

California Current enters the survey area in the north and splits into two branches, one flowing west around a cyclonic eddy centered at  $\sim 200\text{ km}$  offshore, and the other flowing south as a coastal current. This coastal flow is also suggested by the salinity distribution. Near Guadalupe Island the California Current meanders and apparently merges with the coastal flow. There is no evidence for a coastal poleward flow at this depth. Temperatures and salinities were about  $2^{\circ}$  to  $3^{\circ}\text{C}$  and  $0.2\text{--}0.4$  lower than on IMECOCAL cruise 9801 (fig. 20), consistent with the transition to La Niña conditions.

Figures 24 and 25 show vertical distributions of temperature and salinity anomalies for IMECOCAL line 120 (off Vizcaíno Bay) for each cruise. The anomalies are

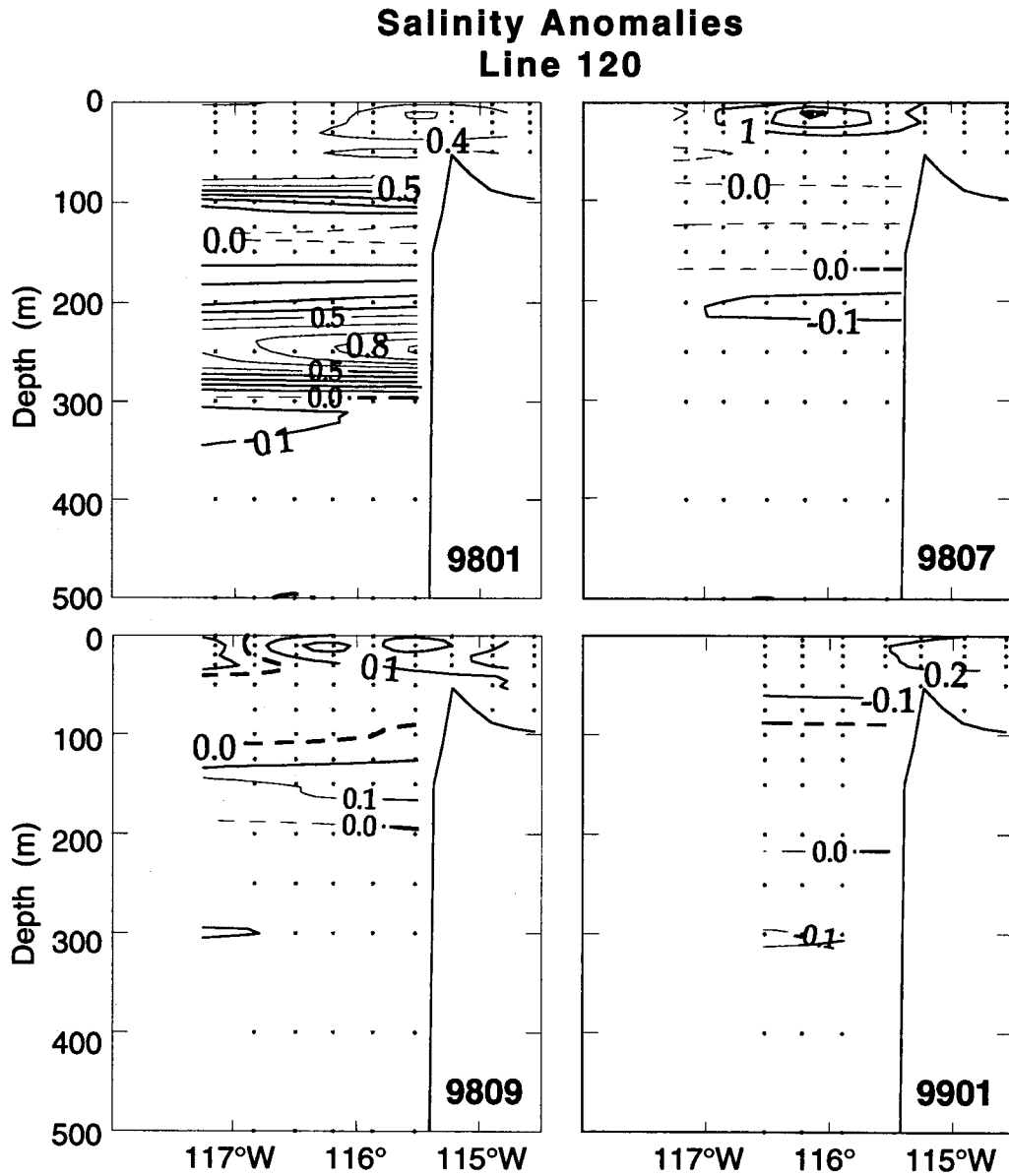


Figure 25. Salinity anomalies for line 120 from IMECOAL cruises 9801, 9807, 9809, and 9901. Anomalies were calculated from mean values given by Lynn et al. (1982) for the period 1950–78.

based on climatological means for the period 1950–78 (Lynn et al. 1982) and may not be directly comparable in magnitude to the anomalies calculated for CalCOFI, which are based upon a longer reference period. In general, temperatures were above the norm on the January and July 1998 cruises, with maximum values of  $5^{\circ}$  over the shelf break at 100 m. July showed positive surface anomalies of up to  $3^{\circ}$ . Both 9809 and 9901 cruises showed  $1^{\circ}$  to  $2^{\circ}$  negative anomalies inside Vizcaíno Bay. Furthermore, cruise 9809 showed positive anomalies in the upper 50 m offshore. Salinity anomalies were relatively small on all of the cruises except for January 1998. Two maxima were observed, one at 100 m and another at 250 m, on cruise 9801.

A similar pattern, but with smaller anomalies, was also observed in October 1997 (Lynn et al. 1998). The upper anomaly maximum (0.5) is at the same depth as the maximum temperature anomaly. The T-S plots (not shown here), suggest that this anomaly layer is found in the core of the California Current. The core is about 20–30 m thick and penetrates offshore as a gradually thickening subsurface lens. The dynamic topography for 100/500 dbar indicates that the California Current flows as an offshore clockwise loop, with southerly flow at this depth. The anomalous core at 250 m is located over the shelf break, and the anomalies reach values of 0.9. This core is associated with a poleward flow of subtropical subsurface water (Wyrki 1967), with salinities

### CalCOFI Cruise Means (1984-1999)

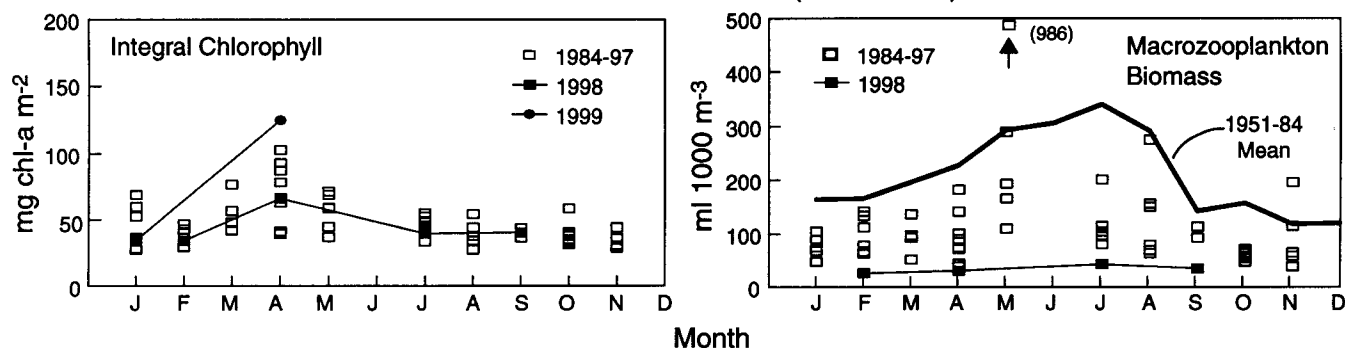


Figure 26. Cruise means of vertically integrated chlorophyll and macrozooplankton biomass plotted versus the month of CalCOFI cruises from 1984 to 1999. Each point represents the mean of all measurements on a cruise (normally 66). The open squares show the cruises that took place from 1984 to 1997. The solid symbols are cruises from 1998 and 1999; cruises from individual years are connected with lines. The bold line in macrozooplankton biomass indicates the monthly means for 1951-84.

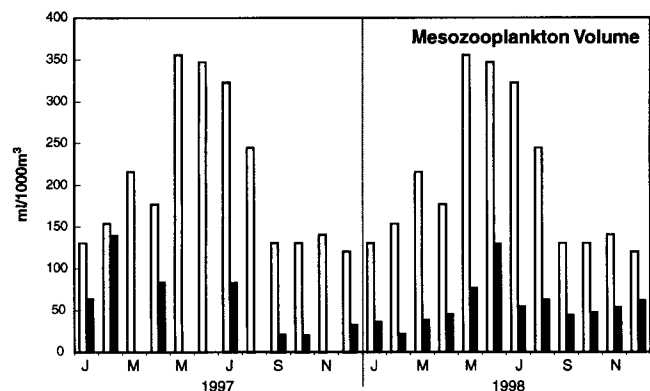


Figure 27. The time series of mesozooplankton volumes for 1997 and 1998. The clear bars represent long-term averages (including recent data) and are repeated for each year. The dark bars represent data for 1997 and 1998. The stations are the nearshore stations out to and including station 60 in the pattern occupied since 1985 between and including lines 77 and 93. Macrozooplankton volumes do not include the volumes of organisms whose individual volume is greater than approximately 5 ml.

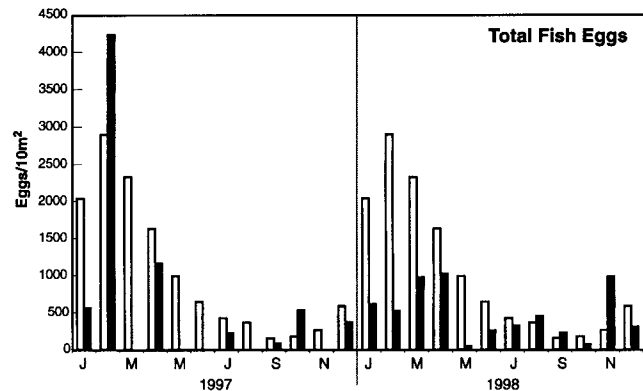


Figure 28. The time series of total fish eggs for 1997 and 1998. The clear bars represent long-term averages (including recent data) and are repeated for each year. The dark bars represent data for 1997 and 1998. The stations are the nearshore stations out to and including station 60 in the pattern occupied since 1985 between and including lines 77 and 93.

above 34.5 and temperatures in the range of 9° to 10°C, extending from 200 to 300 m in the vertical and about 120 km offshore.

#### Ecosystem Structure

The cruise mean plots for vertically integrated chlorophyll and macrozooplankton biomass (fig. 26) include the period of the strong influences of the 1997-98 El Niño and the transition to cool-water conditions (data for chlorophyll only). Chlorophyll followed the pattern of the last decade in that no long-term trend was evident. The vertically integrated values do not look anomalous in the context of data taken since 1984, when systematic time-series measurements of chlorophyll were started by CalCOFI. The April 1999 value was the highest observed since 1984, and this was coincident with the anomalously low temperatures and shallow nutricline seen throughout the study area. Macrozooplankton biomass also continued the long-term trend of decreasing values observed since the mid-1970s (Roemmich

and McGowan 1995; McGowan et al. 1998). The values in 1998 were the lowest since 1984 for each of the cruises. The biomass values for 1999 were not available as this report was being prepared.

CalCOFI plankton samples are routinely sorted for the abundance of fish eggs and larvae in order to provide information about population dynamics of commercially important species. The abundances of macrozooplankton, total fish eggs, sardine eggs, anchovy eggs, and small larvae of hake from the CalCOFI survey cruises and the mini El Niño cruises are shown here (figs. 27-31). The standing crop of total fish eggs ranged from about 1/5 to 1/2 the long-term (1951-98) average from January 1998 to June 1998 (fig. 28). Since hatching time is faster in warm water, the decrease in production will not be as large as implied by the decline in standing stock. But this temperature dependence will, in principle, be small. We do not know the origin of this decline in production. It may be that less fecund fish species moved in from the equatorial side of the study area, or it may be

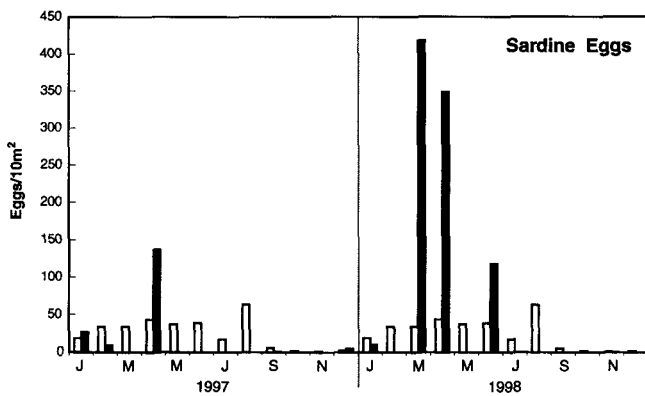


Figure 29. The time series of sardine eggs for 1997 and 1998. The clear bars represent long-term averages (including recent data) and are repeated for each year. The dark bars represent data for 1997 and 1998. The stations are the nearshore stations out to and including station 60 in the pattern occupied since 1985 between and including lines 77 and 93.

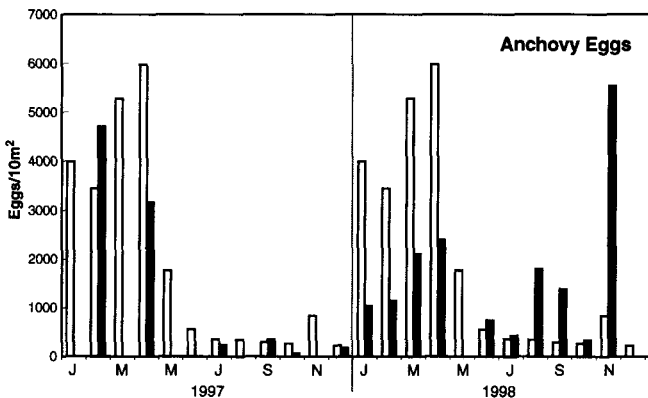


Figure 30. The time series of anchovy eggs for 1997 and 1998. The clear bars represent long-term averages (including recent data) and are repeated for each year. The dark bars represent data for 1997 and 1998. Extrusion of anchovy eggs has been adjusted for the years with 1 m ring nets with 30xxx gauze silk nets (1951-75) and the years with higher-speed bongo nets with 0.505 mm Nitex nylon netting (Loggerwell, pers. comm.). The stations are the nearshore stations out to and including station 60 in the pattern occupied since 1985 between and including lines 77 and 93.

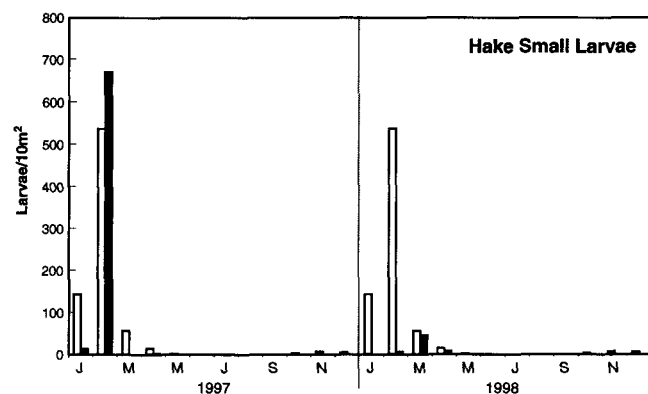


Figure 31. The time series of hake larvae for 1997 and 1998. The clear bars represent long-term averages (including recent data) and are repeated for each year. The dark bars represent data for 1997 and 1998. Extrusion of hake larvae (2 mm-3.75 mm) has been adjusted for the years with 1 m ring nets with 30xxx gauze silk nets (1951-75) and the years with higher-speed bongo nets with 0.505 mm Nitex nylon netting (Loggerwell, pers. comm.). The stations are the nearshore stations out to and including station 60 in the pattern occupied since 1985 between and including lines 77 and 93.

that local fishes produced less spawn. Another possibility is that with warm surface layers, fish normally found within the 0-210 m depths sampled by the bongo net spawned at greater depth, or their eggs sank or did not rise into the sampled layer.

Sardine eggs became more abundant in 1997 and 1998 (fig. 29). The sardine has been increasing in abundance and spawning area since the 1970s, and recent increases are probably more indicative of the long-term trend than a response to El Niño conditions. The low values at the onset of cooler conditions are correlated with the transition to La Niña conditions, but this too should not necessarily be interpreted in terms of a population response, because sardine spawning is normally at a low ebb in the autumn.

Conversely, the anchovy has been decreasing in spawning area in the last two decades, and the trend of low abundance, ranging from  $1/5$  to  $1/2$  normal, may be reflected in addition to a population response to El Niño conditions (fig. 30). The pattern of normally low anchovy egg abundance in autumn and the observed high rate during the fall of 1998 leads to a possibility that the anchovy population is increasing in concert with the transition to La Niña conditions.

The hake population has been remarkably stable in recent years, so the extremely low abundance of the spawn in 1998 is unusual (fig. 31). It is possible that hake spawning shifted to the north during the warm El Niño conditions, as it did during 1984. It is not likely that the low abundance of hake eggs is due to a lack of spawning biomass.

There is a clear need for additional information on the size and depth distribution of the zooplankton, ideally to include smaller sizes in order to better understand how plankton dynamics influence fish populations. To this end, the standard CalCOFI bongo net was augmented with an optical plankton counter (OPC; Herman 1988) beginning with cruise 9802. The OPC counts and estimates the size of particles of about 250 microns equivalent spherical diameter (ESD) and greater by measuring the light they occlude when passing through a fixed beam. The OPC in CalCOFI is mounted in the mouth of the starboard net of the standard bongo frame and is equipped with batteries, an integral flowmeter, and an internal data logger. Data include the number, size, and detection time of particles; flow rate; light attenuation; depth; and time. This new technological approach has the advantage that no additional station time is required to collect the information and that the electronic data can be processed and distributed quickly.

Here we present a representative set of preliminary data from deployments at stations on line 87 for cruises 9804, 9807, 9809, and 9901. The data have been binned over 10 sec intervals and within three size ranges corre-

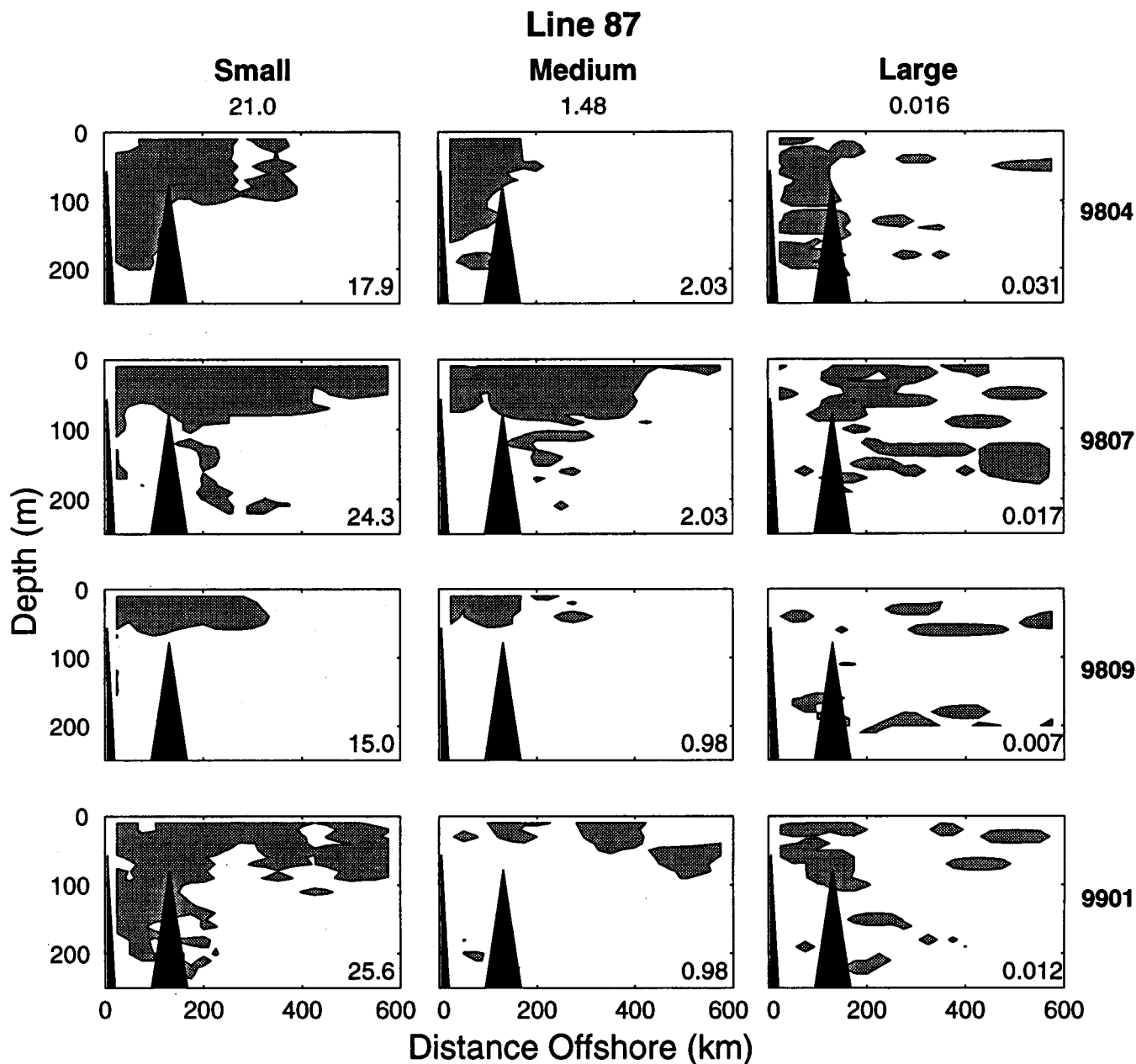


Figure 32. Optical plankton counter (OPC) data for line 87. Shown is particle concentration (particles liter<sup>-1</sup>) for small (0.266–0.722 mm ESD, left panels), medium (0.722–2.38 mm ESD, center panels), and large (2.38–14.0 mm ESD, right panels) particles for four cruises (indicated at right). For each panel, particle concentration is shown in relation to distance offshore and depth. The number at the top of each column of panels is the mean particle concentration for all four cruises for the respective particle size class. The number in the lower right corner of each panel is the mean particle concentration within each cruise for the respective size class. The shaded regions in the panels represent particle concentrations greater than the mean concentration for all cruises for the respective size class.

sponding to (a) particles smaller than quantitatively retained by the CalCOFI 505 micron mesh bongo net (small: 0.266–0.722 mm ESD); (b) most copepods and smaller zooplankters quantitatively retained in the CalCOFI bongo net (medium: 0.722–2.38 mm ESD); and (c) large organisms, e.g., euphausiids (large: 2.38–14.0 mm ESD). The mean concentration (particles liter<sup>-1</sup>) has been computed for each size class over all cruises and within each cruise (fig. 32). Regions within each

cruise where particle concentration was greater than the average for all cruises are also shown in fig. 32 for each size class.

These data are too few to make inferences about interannual variability of the zooplankton in the California Current. But they do indicate the potential of the OPC for addressing this and the larger objective stated above. For example, the distribution and abundance of most (small and medium) particles show surface maxima. Table 2

TABLE 2  
 Optical Plankton Counter Data for Line 87

Cruise	Small:(medium+large) <sup>a</sup>	
	Numbers	Biovolume
9804	8.68:1	0.304:1
9807	11.9:1	0.633:1
9809	15.2:1	0.845:1
9901	25.8:1	1.01:1
Combined cruises	14.0:1	0.599:1

<sup>a</sup>The ratios of small:(medium+large) particles are provided in terms of numbers and biovolume for four cruises separately and combined.

shows the ratio of small:(medium + large) particles sensed on line 87 in each cruise. Also shown are such data for estimated biovolume per liter; in this case, the biovolume of each particle was calculated from its ESD with the equation of Herman (1988). On average, there were 14.0 times more particles smaller than 0.722 mm ESD than particles larger than this, and the ratio varied between cruises (8.68 to 25.8). In terms of biovolume, however, the reverse obtained, with the medium size class containing the greatest biovolume, and on average there being 0.599 as much biovolume in the 0.266–0.722 mm ESD size class as in the 0.722–14.0 mm size class, with similar intercruise variation in this ratio (0.304–1.01). Thus, on average for the data considered here, the CalCOFI bongo net probably captured only a small fraction of the total number but most of the biovolume of particles sensed by the OPC. These preliminary data indicate significant spatial and temporal variation in the abundance and size of the zooplankton and demonstrate our ability to measure it, with potentially significant im-

plications for our understanding of the California Current system and its change.

CalCOFI time-series cruises also provide a continuing opportunity for systematic surveys of the distribution and abundance of seabirds in relation to oceanographic conditions off southern California. Recent surveys during El Niño and the transition to La Niña conditions have facilitated the study of how seabirds respond to interannual oceanographic variability off our coast. Seabird communities off southern California have undergone persistent changes (Hayward et al. 1996; Veit et al. 1996; Hyrenbach and Veit 1999), which appear to be in response to long-term ocean warming and declining zooplankton biomass (Roemmich and McGowan 1995). In addition to these decadal trends, interannual changes in the location of water masses and current systems are known to influence seabird distribution and abundance in the eastern Pacific (Wahl et al. 1989; Ribic et al. 1992; Ainley et al. 1995).

Seabird populations off southern California responded to the recent onset of La Niña conditions during the fall of 1998 in two ways. First, the warm-water species prevalent during the preceding El Niño event were replaced by immigrating subarctic species. For instance, while the black-vented shearwater (*Puffinus opisthomelas*) made up over one-third of all birds recorded during the fall of 1997, its relative abundance dropped to less than 10% in 1998. Conversely, the pink-footed shearwater (*P. creatopus*) increased from 13% to 53% to become the most numerous bird during the fall of 1998 (fig. 33). Most notably, sooty shearwater (*P. griseus*) abundance increased six-fold

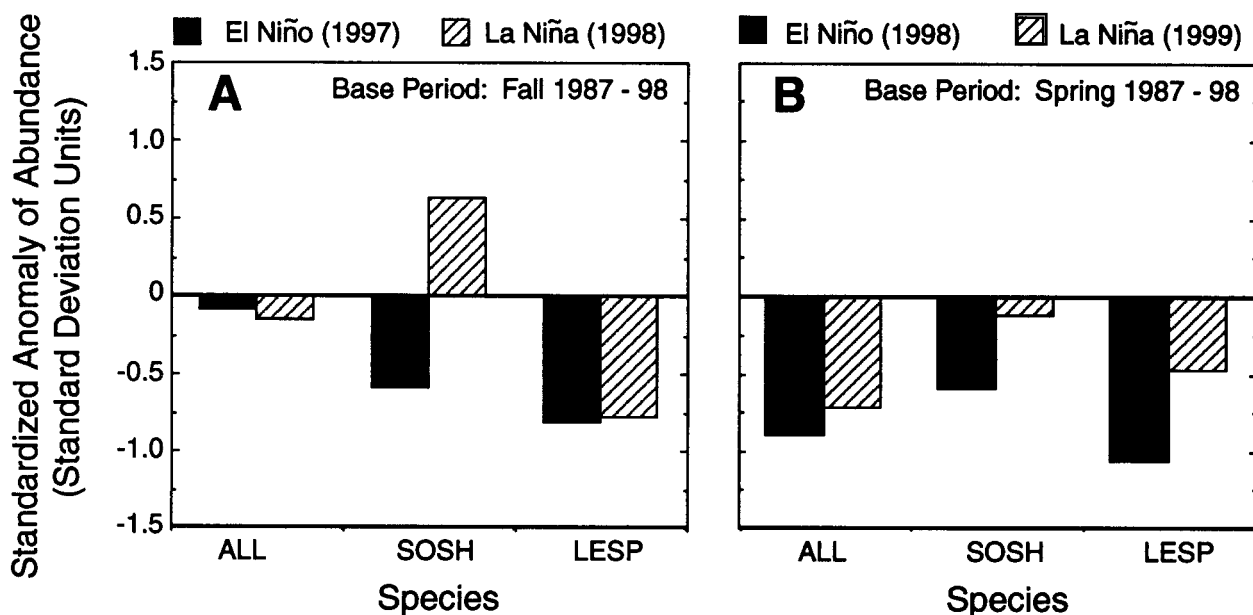


Figure 33. Changes in abundance for all bird species combined (ALL), and for the numerically dominant coastal (SOSH: sooty shearwater) and offshore (LESP: Leach's storm-petrel) seabirds during fall (A) and spring (B). Histograms depict deviations from the long-term seasonal means for cruises in September 1997–98 and April 1998–99.

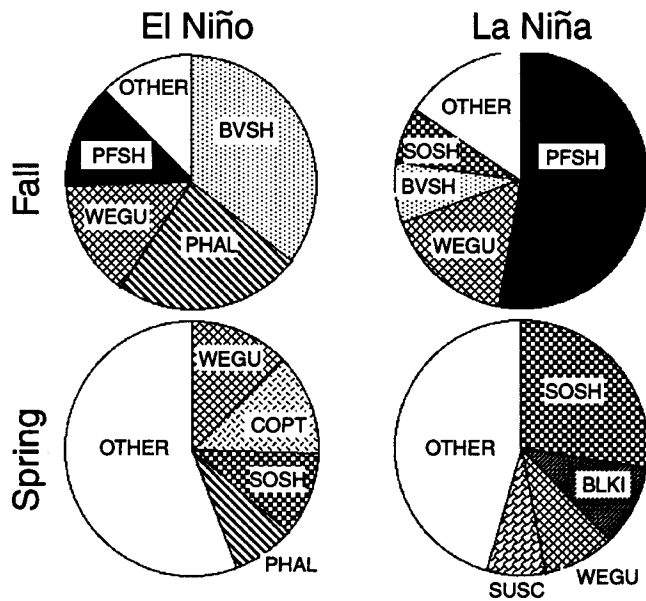


Figure 34. Relative abundance of the four most numerous bird species during El Niño (1997–98) and La Niña (1998–99) conditions. Relative abundance was computed by dividing the number of individuals of a given species by the total number of seabirds sighted during each cruise. BLKI: black-legged kittiwake; BVSH: black-vented shearwater; COPT: Cook's petrel; PFSH: pink-footed shearwater; PHAL: red and red-necked phalaropes; SUSH: sooty shearwater; SUSC: surf scoter; WEGU: western gull.

to soar beyond its long-term seasonal mean for the first time since 1992 (fig. 33). Similarly, the spring avifauna switched from one dominated by Cook's petrels (*Pterodroma cooki*) in 1998 to one dominated by sooty shearwaters and black-legged kittiwakes (*Rissa brevirostris*) in 1999. While the former is a subtropical seabird most abundant in central Pacific and transition zone waters (Wahl et al. 1989), the shearwater and kittiwake are subarctic species whose abundance off California peaks during years of cool ocean temperatures (Ainley 1976; Veit et al. 1996).

Additionally, surveys revealed that total bird abundance during 1998–99 consistently surpassed the levels observed during the 1997–98 El Niño (fig. 34). There were concomitant increases in the abundance of the dominant coastal and pelagic species in fall (fig. 33A) and spring (fig. 33B), though total seabird abundance increased only in spring. It is likely that the emigration of warm-water species in response to cooling conditions caused the decline in total bird abundance in the fall of 1998. This initial decline was offset by the arrival of far-ranging subarctic species during winter and spring.

A preliminary interpretation of these patterns is that shifts in water mass boundaries and large-scale productivity patterns driven by La Niña forcing probably affected seabird distributions off southern California (Ainley 1976; Veit et al. 1996). It is very likely that far-ranging subarctic species migrated into the CalCOFI region in response to cooling ocean temperatures and

increased chlorophyll, while subtropical seabirds shifted their distributions to the south and west. It is unclear, however, whether the 1998–99 La Niña will affect long-term seabird abundance in the CalCOFI region. Years of high upwelling enhance the breeding success of resident seabird populations off central California (Ainley et al. 1995). Yet the demographic effects of these cold-water episodes on far-ranging visitors such as shearwaters and kittiwakes remain unknown. Moreover, data indicate that seabird abundance in the CalCOFI region has continued to decline in recent years, despite substantial variability in ocean conditions (Hayward et al. 1996; Lynn et al. 1998; Hyrenbach and Veit 1999). This observation suggests that the long-term association between seabirds and oceanographic variability off southern California overrides short-term fluctuations driven by interannual forcing.

The ecosystem observations in the CalCOFI study area can be related to biological changes in the region farther to the north. Since 1983, the NMFS/SWFSC Tiburon Laboratory has surveyed juvenile rockfish each spring off central California (36°30'–38°10') to develop a recruitment index. Present sampling includes ADCP, CTD, and chlorophyll. The catches of shortbelly rockfish and all rockfish juveniles from the May–June 1998 survey were the lowest in the history of the survey. Low abundances were apparent for other fish and invertebrate species as well, including normally abundant juvenile hake, squid, and euphausiids. Numbers of seabirds and marine mammals were the lowest since 1984. Juvenile sardines were an exception (Keith Sakuma, Tiburon Lab, pers. comm.). The upper water column was unusually warm (12°–15°C) and fresh (salinity of 32–33). Much of the region was dominated by a lack of upwelling and the onshore displacement of California Current water, while high freshwater discharge from the San Francisco Bay heavily influenced the Gulf of the Farallones. Chlorophyll levels were extremely low.

Few rockfish larvae were found in early 1999. The temperature was cool and the upper layer well mixed compared to previous years. Chlorophyll samples taken at the subsurface maximum layer were low (max = 1.9  $\mu\text{g l}^{-1}$ ). Generally, adult rockfish schools were smaller in comparison to historical data, which tends to corroborate the declining trend in the survival of juvenile shortbelly rockfish seen during the last decade. However, the stomachs of the fish that were collected were full of euphausiids, and they also had large volumes of mesenteric fat. This may lead to increased larval survival this year (David Woodbury, Tiburon Lab, pers. comm.).

The data from the offshore waters collected on CalCOFI cruises can also be related to events in southern California kelp forest communities. Forests of giant kelp (*Macrocystis pyrifera*) in southern California are highly

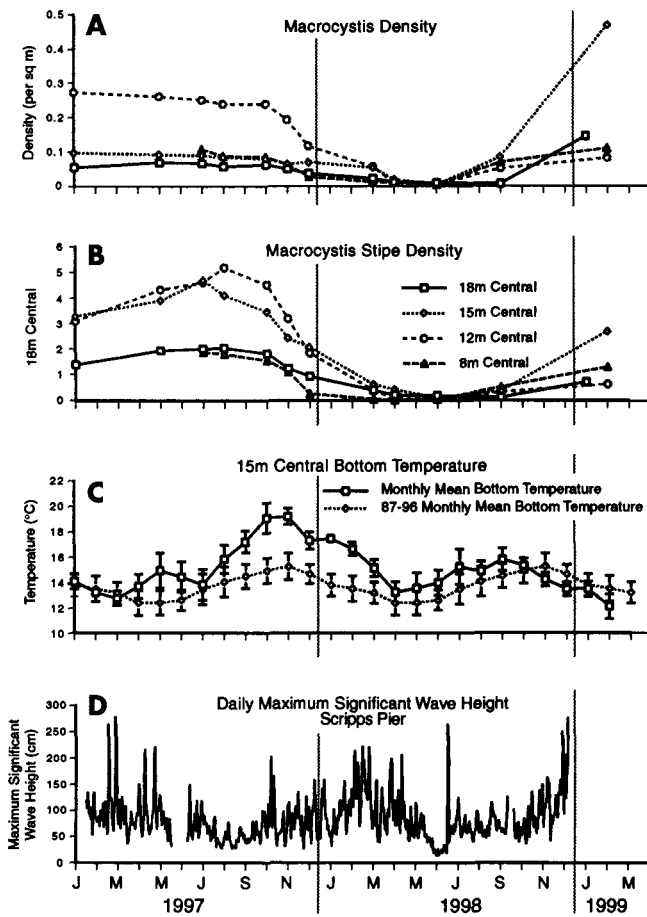


Figure 35. A, Changes in density of *Macrocyctis* adults (defined as having four or more stipes), and B, stipe density for permanent sites at 18, 15, 12, and 8 m in the center of the Point Loma kelp forest, January 1997 through March 1999. See Tegner et al. 1997 for sampling details. C, In situ temperature at 15 m for 1997–99 and the mean for 1987–96; error bars represent one standard deviation. D, Daily maximum significant wave height from the SIO Pier. Gaps in the data are due to equipment failure (Coastal Data Information Program).

dynamic communities that track environmental variability associated with El Niño–Southern Oscillation events. Dependent on high levels of nutrients to maintain growth rates and standing biomass, *Macrocyctis* populations are sensitive to interannual variability in sea-surface temperatures, measured as a surrogate for nitrate availability or stress (Tegner et al. 1996). Because these plants can only store up to a month's worth of nitrogen, there is little lag between ambient conditions and growth rates. Two major and interacting sources of mortality for giant kelp are storm waves and nutrient stress; the severity of the damage caused by storm waves is affected by the nutrient status of the plants (Dayton et al. 1992). *Macrocyctis* mortality is also highly age dependent; two- to three-year-old plants have the highest survival rates at Point Loma (Dayton et al. 1984).

The timing of the very strong El Niño of 1997–98 in the Point Loma kelp forest near San Diego is illustrated by the temperature curve in figure 35. Positive

temperature anomalies peaked in fall 1997 and winter 1998, and continued through the end of summer 1998. By winter 1999, there was evidence of cooler than normal, La Niña conditions. Strong El Niño winters in the Northern Hemisphere are often accompanied by extraordinary storm seasons in southern California. The winter of 1998 produced more than twice as many large wave events, including some with exceptionally long duration, than did the last strong El Niño in 1983 (Seymour 1998). The combination of the storms and warm water led to virtually complete mortality of *Macrocyctis* at Point Loma (fig. 35A). There was recruitment of giant kelps in spring and summer 1998, but warm, nutrient-depleted water during the summer followed by another high-wave-energy winter led to poor growth and survival of young plants, especially at the shallower 12 and 8 m sites. Cold, nutrient-rich waters in winter and spring 1999 are supporting excellent growth of plants that survived the winter. Plant densities will remain low at the shallow sites for the lifetime of these cohorts because of the loss of so many juveniles; densities at the deeper sites will continue to increase as small plants grow to four stipes (analogous to the branches of land plants), our criterion for adulthood. Given the outstanding growth conditions, increased stipe density at the shallow sites has the potential to make up the loss of biomass from density reductions, because plant size is strongly related to temperature/nutrient availability (Tegner et al. 1996).

## DISCUSSION

The fiftieth anniversary of the CalCOFI program is an appropriate time to consider the time-series observations in a larger context. A broad suite of new observational technologies is becoming available. Findings from prior observations are being analyzed and new insights being gained. This may lead to a reconsideration of the priorities for different types of measurements currently being made and new types of measurements that could be made. Here we place the CalCOFI time-series observations in a larger regional context and consider them over longer time scales. We consider the value of the CalCOFI time-series observations for purposes other than the fisheries oceanography focus of CalCOFI, such as their role in supporting policy making and management on both regional and global change space-time scales.

It is clear that CalCOFI needs to continue to consider how well the present sample scheme resolves temporal changes and whether the spatial scale of the sample grid is appropriate to support our basic mission. The present sample pattern (fig. 1) of quarterly cruises done every year was implemented in 1985. This represented a large change in space-time scales from the previous pattern of intensive sampling of a larger area extending from central Baja California, Mexico, to Point Arena;

the pattern was completed over one annual cycle every third year. This change in space–time scale of sampling was based upon the observation that the low–frequency signal is spatially coherent over large spatial scales (Chelton et al. 1982), and upon the need to better resolve seasonal and interannual variability. The suite of properties which were routinely measured was also increased in 1985 to include nutrients, chlorophyll, and primary production as “core” measurements. Additional properties have been added in recent years. This change in the scale of sampling has been successful in that the present pattern does a better job of resolving interannual and seasonal variability. But it can be seen from figures 17, 18, and 26 that the quarterly cruises still do not sufficiently resolve the annual cycle. Annual averages may be biased by hitting or missing what may be a sharp peak, especially during the period of rapid change in biological structure during spring and early summer. CalCOFI scientists are exploring approaches to additional cruises, possibly using continuous sampling technology, in order to better resolve the annual cycle.

CalCOFI researchers have observed (data not shown) that the spawning range of the sardine is expanding to the north. This expansion may be related to increases in the sardine population and changes in physical structure and circulation patterns related to El Niño. The need to sample, at least, the abundance of fish eggs in the region north of the present survey area led CalCOFI to consider the value of sampling three additional lines north of the normal pattern by using continuous sampling technology (CUFES, CUDLS—CalCOFI underway data logging system, and ADCP). This approach has the advantage of obtaining the most critical information at the least cost in ship and technician time. Its drawback is the lack of subsurface physical information, except ADCP, and CalCOFI researchers are exploring additional approaches to make up for this (e.g., seasoar or free–fall CTD systems, which can be deployed from a moving ship). The CalCOFI interest in sampling in the central California region coincides with renewed interest in ocean observing programs by U.S. GLOBEC and other large oceanographic programs.

The theme of applying new technological approaches to address longstanding questions is capturing increasing interest within CalCOFI as well as at the national and international levels. New technologies have the potential to provide new types of information (e.g., CUFES or OPC) or a more efficient way to gather the same type of information that is already being collected (e.g., replacement of Nansen bottle casts with CTD or seasoar profiles). When methodologies change, CalCOFI has generally been very conservative in its approach to implementing them in order to ensure the continuity of the time series. Detection of long–term trends requires

that data sets be taken with comparable techniques. However, new technologies—especially those such as OPC, ADCP, and CUFES, which do not require additional station time—have great potential. CalCOFI researchers will continue to evaluate the design of the sample program to provide the best and most efficient approach to meeting information needs. The perception of the value of specific observations may also change as new understanding is gained. Such new understanding may also lead to changes in programmatic priorities. CalCOFI has encouraged participation by a wide range of cooperative research projects, thus providing a cost-effective opportunity for the development of new technologies and an opportunity to evaluate the operational value of new information.

In addition to supporting the basic programmatic objectives of CalCOFI, the observations gathered in the time–series program have great value for a broad range of other uses. Although meeting the core objectives of CalCOFI must take precedence in setting priorities for alternative sampling schemes, CalCOFI can share its time–series observations with other programs and would like to see such programs expand. There is renewed interest at the state, national, and international levels in ocean observing systems. The coastal ocean is highlighted as a region needing special attention. CalCOFI, due to its long historical record and the broad suite of properties which have been measured, will be an important component of an integrated observing system. The CalCOFI data have great potential value for supporting more broad policy and management objectives than the fisheries oceanography objectives that are central to CalCOFI. However, the use of the data may not reach its full potential because the data products developed in support of CalCOFI objectives may not be sufficiently focused to meet information needs in other policy and management areas. This is also an area in which CalCOFI would like to grow in the future.

Management and policy issues can be considered on at least two space–time scales. The first is the regional and local areas which are included within the CalCOFI survey area. CalCOFI is continuing to expand its collaboration with research programs focusing on kelp forest and “nearshore” ecosystems. One challenge here is for CalCOFI to make better use of the higher–frequency data collected at coastal buoy and shore station sites (e.g., figs. 5, 6, 8, 9, and 35), and, in turn, learning to what extent the findings of CalCOFI apply to these other ecosystems. The nature of the scientific and management issues differs to some extent in the nearcoastal region, and additional work will have to be done in order to directly apply CalCOFI observations to management and policy needs. There is more of an emphasis on ecosystem management and the processes occurring at the land–

ocean interface than on fisheries oceanography issues. A large fraction of the observational effort is devoted to compliance monitoring (e.g., sampling around ocean discharges covered by a National Pollutant Discharge Elimination System permit to ensure compliance with the terms of the permit). Additional observations are made in support of basic research within this general region. Greater consideration of the results of the CalCOFI time-series observations would allow regional policy makers to place the results of local or point source compliance monitoring in a regional context. It may be necessary to develop additional types of data products which are more focused upon the needs of regional policy makers in order to increase the value of the CalCOFI data for such issues.

CalCOFI data will also be applied to studies of ecosystem change on global and climate change time-space scales. Here the CalCOFI observations will be considered as one component of a global monitoring system. Many of the changes in the California Current ecosystem documented by CalCOFI are correlated with climate-scale changes in the atmosphere and physical structure of the ocean (Chelton et al. 1982; Roemmich 1992; Roemmich and McGowan 1995; Veit et al. 1996; McGowan et al. 1998). CalCOFI observations will have great value in testing and developing new models linking climate change and physical structure. CalCOFI will benefit from the development of such models because the progress in predicting physical structure based upon observations or models is clearly proceeding more rapidly than predictive models of ecosystem structure. In particular, the CalCOFI region seems to be a natural region for the development and evaluation of assimilation models of ocean circulation. The ongoing time-series observations will be ideal as data inputs for such models and for testing the results. CalCOFI will benefit from an improved knowledge of the circulation, since the strong correlations between physical and biological structure in the region have been well established.

## ACKNOWLEDGMENTS

We thank all of the contributing research programs for their extra efforts in processing and analyzing their most recent data so that they could be included here. We again wish to particularly acknowledge the ships' crews, research technicians, and volunteers whose skill and hard work made this report possible.

## LITERATURE CITED

- Ainley, D. G. 1976. The occurrence of seabirds in the coastal region of California. *West. Birds* 7:33–68.
- Ainley, D. G., W. J. Sydeman, and J. Norton. 1995. Upper trophic level predators indicate interannual negative and positive anomalies in the California Current food web. *Mar. Ecol. Prog. Ser.* 118:69–79.
- Bakun, A. 1973. Coastal upwelling indices, west coast of North America, 1946–71. U.S. Dep. Commer., NOAA Tech. Rep., NMFS SSRF-671, 103 pp.
- Chelton, D. B., P. A. Bernal, and J. A. McGowan. 1982. Large-scale interannual physical and biological interaction in the California Current. *J. Mar. Res.* 40:1095–1125.
- Dayton, P. K., V. Currie, T. Gerrodette, B. D. Keller, R. Rosenthal, and D. Ven Tresca. 1984. Patch dynamics and stability of some California kelp communities. *Ecol. Monogr.* 54:253–289.
- Dayton, P. K., M. J. Tegner, P. E. Parnell, and P. B. Edwards. 1992. Temporal and spatial patterns of disturbance and recovery in a kelp forest community. *Ecol. Monogr.* 62:421–445.
- Hauray, L. R., E. Venrick, C. L. Fey, J. A. McGowan, and P. P. Niiler. 1993. The Ensenada Front: July 1985. *Calif. Coop. Oceanic Fish. Invest. Rep.* 34:69–88.
- Hayward, T. L., and A. W. Mantyla. 1990. Physical, chemical and biological structure of a coastal eddy near Cape Mendocino. *J. Mar. Res.* 48:825–850.
- Hayward, T. L., and E. E. Venrick. 1998. Nearsurface pattern in the California Current: coupling between physical and biological structure. *Deep-Sea Res.* 45:1617–1638.
- Hayward, T. L., S. L. Cummings, D. R. Cayan, F. P. Chavez, R. J. Lynn, A. W. Mantyla, P. P. Niiler, F. B. Schwing, R. R. Veit, and E. L. Venrick. 1996. The state of the California Current in 1995: continuing declines in macrozooplankton biomass during a period of nearly normal circulation. *Calif. Coop. Oceanic Fish. Invest. Rep.* 37:22–37.
- Herman, A. W. 1988. Simultaneous measurement of zooplankton and light attenuation with a new optical plankton counter. *Cont. Shelf Res.* 8:205–221.
- Hyrenbach, K. D., and R. R. Veit. 1999. Response of seabird abundance to long-term changes in the California Current, 1987–98. Pacific Seabird Group Meeting, 24–28 February 1999. Blaine, Washington. Abstract.
- Kalnay, E., and coauthors. 1996. The NCEP/NCAR reanalysis 40-year project. *Bull. Amer. Meteorol. Soc.* 77:437–471.
- Lynn, R. J., K. A. Bliss, and L. E. Eber. 1982. Vertical and horizontal distributions of seasonal mean temperature, salinity, sigma-t, stability, dynamic height, oxygen and oxygen saturation in the California Current, 1950–1978. *Calif. Coop. Oceanic Fish. Invest. Atlas* 30, La Jolla, Calif., Scripps Institution of Oceanography, 513 pp.
- Lynn, R. J., F. B. Schwing, and T. L. Hayward. 1995. The effect of the 1991–93 ENSO on the California Current system. *Calif. Coop. Oceanic Fish. Invest. Rep.* 36:57–71.
- Lynn, R. J., T. Baumgartner, J. Garcia, C. A. Collins, T. L. Hayward, K. D. Hyrenbach, A. W. Mantyla, T. Murphree, A. Shankle, F. B. Schwing, K. M. Sakuma, and M. J. Tegner. 1998. The state of the California Current, 1997–1998: transition to El Niño conditions. *Calif. Coop. Oceanic Fish. Invest. Rep.* 39:25–49.
- McGowan, J. A. 1985. El Niño 1983 in the Southern California Bight. In *El Niño North; El Niño effects in the eastern subarctic Pacific Ocean*, W. S. Wooster and D. L. Fluharty, eds. Washington Sea Grant Program, Univ. Washington, Seattle, pp. 166–184.
- McGowan, J. A., D. R. Cayan, and L. M. Dorman. 1998. Climate-ocean variability and ecosystem response in the northeast Pacific. *Science* 281:210–217.
- Murphree, T., and C. Reynolds. 1995. El Niño and La Niña effects on the northeast Pacific: the 1991–1993 and 1988–1989 events. *Calif. Coop. Oceanic Fish. Invest. Rep.* 36:45–56.
- NCEP. National Centers for Environmental Prediction. 1997a. Climate diagnostics bulletin, July 1997. Climate Prediction Center, NOAA/NWS/NCEP. No. 98/7. 80 pp.
- . 1997b. Climate diagnostics bulletin, December 1997. Climate Prediction Center, NOAA/NWS/NCEP. No. 97/12. 78 pp.
- . 1998a. Climate diagnostics bulletin, April 1998. Climate Prediction Center, NOAA/NWS/NCEP. No. 98/4. 82 pp.
- . 1998b. Climate diagnostics bulletin, September 1998. Climate Prediction Center, NOAA/NWS/NCEP. No. 98/9. 79 pp.
- . 1998c. Climate diagnostics bulletin, December 1998. Climate Prediction Center, NOAA/NWS/NCEP. No. 98/12. 81 pp.
- . 1999. Climate diagnostics bulletin, March 1999. Climate Prediction Center, NOAA/NWS/NCEP. No. 99/3. 80 pp.
- Nitta, T. 1987. Convective activities in the tropical western Pacific and their impact on the Northern Hemisphere summer circulation. *J. Meteorol. Soc. Jpn.* 65:373–390.

- Reynolds, R. W., and T. M. Smith. 1995. A high resolution global sea surface temperature climatology. *J. Clim.* 8:1571–1583.
- Ribic, C. A., D. G. Ainley, and L. B. Spear. 1992. Effects of El Niño and La Niña on seabird assemblages in the equatorial Pacific. *Mar. Ecol. Prog. Ser.* 80:109–124.
- Roemmich, D. 1992. Ocean warming and sea level rise along the southwest United States coast. *Science* 257:373–375.
- Roemmich, D., and J. McGowan. 1995. Climatic warming and the decline of zooplankton in the California Current. *Science* 267:1324–1326.
- Schwing, F. B., M. O'Farrell, J. M. Steger, and K. Baltz. 1996. Coastal upwelling indices, west coast of North America, 1946–95. U.S. Dep. Commer., NOAA Tech. Memo. NOAA-TM-NMFS-SWFSC-231, 207 pp.
- Schwing, F. B., T. L. Hayward, T. Murphree, K. M. Sakuma, A. S. Mascarenas Jr., A. W. Mantyla, S. I. Castillo, S. L. Cummings, F. P. Chavez, K. Baltz, and D. G. Ainley. 1997. The state of the California Current 1996–1997: mixed signals from the tropics. *Calif. Coop. Oceanic Fish. Invest. Rep.* 38:22–47.
- Scripps Institution of Oceanography. 1999. Physical, chemical, and biological data report, CalCOFI cruises 9707, 9709 and 9712. SIO Ref. 99-5.
- Seymour, R. J. 1998. Effects of El Niños on the West Coast wave climate. *Shore and Beach* 66:36.
- Strub, P. T., P. M. Kosro, A. Huyer, K. H. Brink, T. L. Hayward, P. P. Niiler, C. James, R. K. Dewey, L. J. Walstad, F. Chavez, S. R. Ramp, D. L. Mackas, M. S. Swenson, L. Washburn, J. A. Barth, R. R. Hood, M. R. Abbott, D. C. Kadko, R. T. Barber, D. B. Haidvogel, M. L. Batteen, and R. L. Haney. 1991. The nature of cold filaments in the California Current system. *J. Geophys. Res.* 96:14,743–14,768.
- Tegner, M. J., P. K. Dayton, P. B. Edwards, and K. L. Riser. 1996. Is there evidence for long-term climatic change in southern California kelp forest communities? *Calif. Coop. Oceanic Fish. Invest. Rep.* 37:111–126.
- Tegner, M. J., P. K. Dayton, P. B. Edwards, and K. L. Riser. 1997. Large-scale, low-frequency oceanographic effects on kelp forest succession: a tale of two cohorts. *Mar. Ecol. Prog. Ser.* 146:117–134.
- Veit, R. R., P. Pyle, and J. A. McGowan. 1996. Ocean warming and long-term change in the pelagic bird abundance within the California Current system. *Mar. Ecol. Prog. Ser.* 139:11–18.
- Wahl, T. R., D. G. Ainley, and A. R. DeGange. 1989. Associations between seabirds and water-masses in the northern Pacific Ocean in summer. *Mar. Biol.* 103:1–11.
- Walker, P. W., D. M. Newton, and A. W. Mantyla. 1994. Surface water temperatures, salinities, and densities at shore stations. United States west coast. SIO Ref. 94-9.
- Wolter, K., and M. S. Timlin. 1998. Measuring the strength of ENSO—how does 1997/98 rank? *Weather* 53:315–324.
- Wyrki, K. 1967. Circulation and water masses in the eastern equatorial Pacific Ocean. *J. Oceanol. Limnol.* 1:117–147.